DV3.2 Stress and burial history impact on present day state

Organisation(s)   NGI, BGS, NTNU, Geus,

Author(s)   Lars Grande, Elin Skurtveit, Rob Cuss, Rao Martand Singh, Henrik Vosgerau

Reviewer   Daniel Roberts

Type of deliverable   Report

Dissemination level   SHARP Consortium only

WP   3

Issue date   29th-September 2023

Document version   Draft v01b_for SHARP web site

Keywords: CO_2 storage, stress history, stress ratio, consolidation, permeability.

Summary:

This report documents the work done in WP3.2-Stress and burial history impact on present day state. From existing databases, literature data and dedicated rock deformation experiments we have analysed, developed, and tested empirical relationships of K_0, permeability and consolidation parameters vs. stress loading and unloading. The analysis in this report is based on a wide range of datasets applicable for North Sea sedimentary systems including new tests and data from Horda platform and analogues for Endurance site. The results and methodology have general applications, and examples of the relevance are shown for mature Horda Platform area and for the less mature Lisa (DK) at the end of report. This work is input to WP1.2 and 1.3 and are closely linked to DV1.2 report, where, this report documents the experimental testing and empirical relationships.

Contents

Appendix

Appendix A- Mineralogy, deformation and permeability data in Horda Platform (restricted for SHARP, until publlication)

1   Introduction

This report documents the work done in WP3.2, focusing on the impact of lithology and burial history on the present day state of stress. We have analysed existing databases, literature data and dedicated rock deformation experiments to develop empirical relationships between ratio of effective stress ratio (K_0), permeability and consolidation parameters vs. stress loading and unloading. The coefficient of earth pressure at rest, K_0, is defined as the ratio of the effective horizontal stress to the effective vertical stress $K_0 = \sigma_h'/\sigma_v'$. Existing datasets applicable for North Sea sedimentary systems have been reviewed and updated with new tests and data from the Horda platform and analogues for Endurance site. The data selection was based on the availability of released datasets, cores and field stress data, and the Horda platform is the main study area as it is the most mature field. The results and developed methodology have been tested and believed to have general practical applications to areas where less stress data are available. Examples of the methodology for the less mature Lisa structure (DK) are given at the end of this report and in DV1.2 report.

Shallow geotechnical data from Troll and Oseberg in the Horda platform, Northern North Sea was analysed to establish relationships between index parameters and K_0, constrained modulus and permeability. Natural clay, mudstone and shales from various burial depths have been compared with the published datasets. The purpose of test program is to update empirical relationships to evaluate minimum horizontal stress via K_0 based on lithology and mineralogy. This analysis of laboratory data is input for WP1 in developing and calibrating the constitutive model for evaluating sediment compaction erosion and uplift, and glacial loading and unloading. The application and calibration with field stress data are presented in the DV1.2 report, with the main focus for the Horda platform site, where calibration points in terms of XLOT data released from Equinor and supplemented with LOT data.. The review, testing and analysis presents general relationships with wide application for CCS sites. The work is performed in collaboration with WP1, and the field stress dataset from XLOT and LOT data have been used to constrain the laboratory test procedures and testing results from empirical relationships.

This report DV3.2 primarily focuses on the laboratory-based results and relationships. These results are aligned with SHARP report DV1.2, where datasets and empirical relations from laboratory are applied with field data for testing and calibration of constitutive model and empirical relations with field stress data.

This report covers worked performed under three subtasks:

<u>Task a (NGI):</u> Consolidation history assessment from soil and rock tests. This task analyses existing database and literature that address the impact of stress history on effective stress ratio (K_0), permeability and compressibility in relation to original sediment composition, mineralogy, clay content and plasticity index. Oedometer test and triaxial K_0 test from both sedimentary layers and geotechnical site investigations have been evaluated to cover the range from loosely mechanically compacted sediments at a shallow depth to the chemically altered rocks from diagenesis processes. Parts of the work are also reported and presented in GHGT-16 (Grande et al. 2022), where workflow for estimation of K_0 and minimum horizontal stress based on rock physics relationship of clay content (V_{cl}), smectite content, over-consolidation ratio (OCR) and well log data are presented in more detail. The workflow was established and tested on wells in the Smeaheia, Aurora and Troll areas as part of SHARP project WP3.2 and

WP1.2 integrated tasks. In this report K_0 test data from natural clays, mudstones and rocks have been included and compared with published datasets with know mineralogical composition to evaluate similarities and differences in K_0 during loading and unloading for non-cemented vs. cemented clays and mudstones. New relationships on K_0 and modulus from clay content have been developed from released geotechnical data from Oseberg and Troll. Existing and new relationships for K_0 are tested and compared with field stress data in report DV1.2 mainly based on data from Horda platform. General methodology are also applied for the less mature Lisa field in Denmark.This report documents relevant mineralogy data from Lisa field and report DV1.2 presents the LOP vs. depth trends.

Task b (NGI/NTNU): Additional test program for geotechnical properties, including plasticity index (Ip) and friction angle of remoulded material of reconstituted caprock Drake from Eos well 31/5-7, was done to test the empirical relationship for K_0. Furthermore, triaxial K_0 testing to study site-specific effects of mineral and clay and load history has been done on shallow onshore cores from the analogue site of Onsøy, which is also representative of the Quaternary clays in the Troll and Horda Platform area. Results have been compared with in situ field stress measurements in Onsøy, and experience is applied in the simulation of representative quaternary units in the Troll field with PLAXIS. Relevant soil characteristics and stress history have been implemented for the Quaternary units, including the standard Soft Soil Creep model and a new model.

Task c (BGS): Assessment of permeability as a function of both stress history as well as expected future pressure/stress changes related to CO2 storage was tested at BGS. Tests on representative samples of reservoir and caprock representative of those present in the Greater Endurance area will be undertaken using the pore-pressure oscillation technique to get derive functions of permeability and storage versus confining pressure. Two test was completed before this report, one of these were sucscssful and the full results is included in this report. The test included here is on Staithes sandstone representing a reservoir rock. It is planned to conduct the four tests on analogues for reservoir rock (Staithes and Bestwood Sandstone) before moving to the analogue for caprock material (Mercia mudrock), which will take significantly longer time to conduct. If time permits, loose sand will be tested. These tests will be reported when completed as an attachment to DV3.2 or DV3.3 report.

2 Consolidation history assessment from soil and rock tests

Framework for constitutive modelling have been developed under WP1 based on the dataset on synthetic mudstones with known mineralogy from Mondol et al., 2009, Grande et al., 2011, 2013. These developments have been reported in SHARP reports DV1.1b and DV1.2. A workflow to estimate minimum horizontal stress based on the rock physics relationship of clay content (V_{cl}), smectite content and over-consolidation ratio (OCR) and well log data has been established as part of SHARP project under WP3.2 and WP1.2 (Grande et al. 2022). Furthermore, a detailed evaluation of rock rheology for the Horda Platform has been addressed for the purpose of modelling the E-W cross-section through Horda platform. These cover depths from shallow sea surface based on geotechnical wells to the deepest wells in the area (i.e. 0- 3.7km). Correlations have been established and applied to logs. These results have been presented under

Appendix B. Parts of this work have also been presented in the abstract and conference (Grande et al., 2022b).

This method of performing K_0 tests on synthetic clays or reconstituted samples of shales based on original sediment composition from an initial loose state has been found to reproduce rock physics relationships for velocity and permeability vs. stress, and field stresses quite well not only for geotechnical depths but also for sediments at larger burial depths within depth of mechanical compaction (Mondol 2007, 2009 and Grande et al 2011 and 2013). K_0 testing on cemented shales on the other hand, often give to low values of K_0 during initial loading and very high stresses are typically needed to bring sample to stable K_0 representative of normally consolidated state. This is due to the fact that cementation gives a "pseudo pre-consolidation", not generated from grain framework stiffening from chemical processes (Nygård et al 2006). In this chapter K_0 test from natural clays, mudstones and rocks have been compared with published data on clays and sands with various mineralogical composition to evaluate similarities and differences during loading and unloading.

2.1   Introduction

This chapter further elaborates on the empirical relationships presented in Grande et. al (2022) as well as new relationships by including more data into the figures and correlations to constrain the model further and discuss uncertainties.

The coefficient of earth pressure at rest, K_0 (σ_h'/σ_v'),was first introduced by Donath (1891) as the ratio of horizontal stress to vertical stress under a condition of zero lateral strain. The subsequent significant work on K_0 was performed by Terzaghi (1920 and 1925). Over the years, geotechnical engineers have relied mostly on empirical relationships and systematic laboratory tests on sands and clay to assess K_0 for a wide range of soils i.e: Jaky (1944), Kenney (1959), Brooker and Ireland (1965), Massarsch (1979) and Mayne and Kulhawy (1990). Several new relationships have been established based on a series of multivariable regression analyses, including published data and new data on Norwegian clays L'Heureux, 2017.

These existing correlations primarily relate to the effective friction angle φ (effective angle of shearing resistance) of sediments or a combination of plasticity index (Ip) to characterize the plasticity of clays and over consolidation ratio (OCR), which is the ratio between effective vertical stress σ_v' at maximum burial depth and present depth. Both are standard physical index parameters for geotechnical engineering and are widely used onshore and offshore. However, these parameters are not usually available in the petroleum industry for more lithified lithologies at deeper depths. A further evaluation based on the content of clay (V_{cl}) and smectite, which is more commonly known, has been introduced to test the approach for deeper depths and link it to geophysical logs (Grande et al. 2022).

Once K_0 is established, σ_h can be determined from the σ_v' and pore pressure (PP), which through effective stress relations ($\sigma_h = K_0 \cdot \sigma_v' + PP$). The total vertical stress σ_v is a function of the density of overburden from integration of the density log and is most often well constrained for an area.

The method based on laboratory measurements has limitations in correctly determining K_0 in-situ, because other factors potentially affecting the development of σ_h' may

include, for example, earlier stress and strain history, mineralogy, cementation, aging, weathering, pore water fluid, temperature and cementation (Mayne and Kulhawy 1990). These limitations for using uniaxial strain tests from consolidated rocks directly for deeper engineering applications have also been argued by several authors (Mayne and Kulhaway, 1990, Berre et al.,1995, Bjørlykke and Høeg, 2004, Nygård et al. 2004, Andrews and de Lesquen, 2019). K_0 tests on shales have limitations due to over-consolidation from diagenesis at greater depth (>2-2.5km), and the K_0 response in shale below their pre-consolidation stress (Pc') can be strongly affected by the altered texture and mineralogy (i.e., cementation) and core damage effects from unloading during core retrieval as demonstrated for sandstones (Holt et al., 1994).

2.2 Review of K_0 and empirical relationship from laboratory testing

Tables 1 and 2 give an overview of K_0 testing and empirical relations from literature with a focus on mineralogical content and K_0 ratio. The tables include synthetic clays, natural clays and sands, and mudstone and shales. These data have been further evaluated and analysed with a combined dataset in this report. The table is not complete but give an overview of the earliest fundamental studies and later main works at NGI.

Empirical relations from the laboratory have been tested with stress test data from various methods in geotechnical sites in several papers both offshore and onshore, and field tests methods includes the flat dilatometer test (Marchetti 1980, Marchetti et al., 2001), self-boring preussuremeter test and large in-situ plate test (Marsland A, Randolph MF., 1977), field vane test (Aaas et al., 1986). Experiences from offshore tests are from North Sea are summarized in NGI 1990, and ca 10 tests are from Troll (during site investigations in 1987, 1988, 1989) using Fugro McClelland Packer system as well as Marchetti Dilatometer test (Lunne et al., 2006). NGI have experience from testing various methods onshore in various tests sites including Drammen (Lunne et al., 2002, Gundersen et al., 2019).

The objective of further work has been to constrain these relationships by combining existing laboratory data from geotechnical site investigations in the Horda Platform area. Synthetic mixtures of clays with well-known mineralogy have been used as references (from Grande 2011 and 2013). This dataset is the same as that used to develop the constitutive model in SHARP WP1, and these data are also presented in DV1.1 and DV1.2 reports. It should be mentioned that this dataset was part of a larger study also focusing on rock physics relationships including stress dependent permeability and ultrasonic velocity including anisotropy (Mondol, 2009 and 2011).

Table 2-1 K_0 data from literatures. Mineralogy data are coded; Q=quarts, Ca=Calcite, Ill=Illite, Ka=Kaolinite, Chl=Chlorite, Mo=Montmorillonite, Mu=Muscovite, Sm=Smectite, Fe=Feldspar, Ca=Calcite, ML=Mixed layer minerals. Wi=water content, d=density. Vcl=volume clay, Ip=plasticity index. Depth references; D_c = Current Depth, D_m = Maximum burial depth,

Material	Clay and shale	Description and Mineralogy (%)	Vcl %	Ip %	Sm [4] %	K_0	Reference
Natural clays- Reconstituted	Chicago clay	Q=20, Ca=15, Ill=40, Chl=20, Mo=5%	65	10.3	6	0.48	Brooker and Ireland 1965
	Goose Lake Fleur	Q=20-25, Ka=65, Ill=10-15	80	15.6	0	0.51	
	Weald Clay	Q=30, Chl=30, Ill=15, Ka=15, Mo=10%	70	20.6	10	0.54	
	London Clay	Q=15, Chl & Ka=35, Ill=35, Mo=15	85	38.4	15	0.68	
	Bearpow shale	Q=30, Fe=5, Ka=5, Mo=60	65	78.0	60	0.70	
	St. Hilaire Clay	Ill=55, Chl=39, Sm=6	32	23	6	0.55	Mesri and Hayat, 1993
	St.Esprit	Ill=56, Chl=40, Sm=4	19	27	4	0.56	
Synthetic clays and shales	Artificial clay shale	Ill/Mu and ka, Wi=12%, d=2.17g/cm3	-	30	-	0.64 (0.90) [1]	Berre et.al.1995
	Synthetic clays and clays	Mixtures of silt, illite, kaolinite and smectite	30-100		0-50	0.47-0.74	Grande et al. 2011, 2013 and 2023
Mudstones and Shales	Cemented shale	Ill/Mu, Ka, Swelling minerals, wi=3.5%, d=2.16g/cm3	-		-	0.58 (0.35) [1]	Berre et.al.1996
	Kimmeridge clays	Kimmeridge Westbury Clay (**KWC**): Sm 20, Ill/mi 25 , Kaol 10, Q 25, Ara>5, Ca 15, Py 5:	55	39	20	0.77	Nygård et al 2006
		Kimmeridge Bay Clay (**KBC**); Sm 10, Ill/mi 20 , Kaol 30, Q 30, Ca>5 Py >5	65	23	10	(0.7)[1]	
	Draupne (Ling depression)	Q+Fe=40, (Clay frac: Ka=62.1, Chl=0.7, Ill/Mi=19.3, Sm=18)	50.7		18	0.55 [2]	Zadeh et.al. 2017
	Hekkingen	Q+Fe=27, (Clay frac=Ka=47, Ill/Mi=32, Sm=2)	61.0		2	0.54 [2]	

[1] Unload in parenthesis

[2] The reported values are at end of consolidation, may not be entirely stabilized, use with caution

[3] The reported values are at end of consolidation, <u>not stabilized</u>, values should not be used

Mineralogy data from a few key of Lista, Shetland Draupne and Drake units are in Horda Platform is tabulated in Appendix A. Thes data are basis for discussions. For a reference, published data are included here for Drake and Draupne Fm's. The lower unit (Unit IV) from Troll site investigation from Oligocene age (Tertiary) at a depth of ca 220 m TVD bsf has Vcl (<2um) of 38%, whereof 60% of Smectite, 20% Kaolinite, and 20% Illite (Lunne et al., 2006), and this unit may be characterized as Smectitic mudstone. For Drake shale, the bulk content of main clay minerals are; Kaolinite 5-20%, Illite 17-62%, and Smectite 1-9%. The Intra-Drake has more Illite and Smectite compared to the Drake upper and lower units with the following; Kaolinite 8-10%, Illite 59-62%, and Smectite 6-9% (Thompson et al., 2021a, Grande et al., 2022). XRD data from one depth in Drake shale are also available, indicating lower clay content of 61% compared to QEMSCAN value of 85% from the same depth (Grande et al., 2022). For Draupne shale, V_{cl} and TOC are reported to V_{cl}= 66 and 70% and TOC= 2.78 and 2.81 for Alpha and Beta well, respectively (Rahman et al., 2020).

Table 2-2 Overview of equations from various studies and materials. φ = friction angle, Ip=Plasticity index, OCR=Over Consolidation Ratio, Vcl= volume clay

Eq.	Equation	Type of material	Reference
1	$K_0=1-sin\varphi'$	Cohesionless soils	Jaky, 1944
2	$K_0=0.95-sin\varphi'$	Cohesive soils, Reconstituted natural clays	Brooker and Ireland 1965
3	$K_0= 0.45(Ip)^{0.06} OCR^{0.43}$	Brooker and Ireland dataset	L'Heureux et. al., 2017
4	$K_0 = 0.33(Ip)^{0.17} OCR^{0.39}$	Brooker and Ireland dataset, OCR<8	
5	$K_0= 0.49(Ip)^{0.02} OCR^{0.475}$	Norwegian clays, OCR 1-32	
6	$K_0= 0.40(Ip)^{0.08} OCR^{0.47}$	Norwegian clays, OCR<8	
7	$K_0= 0.48(Ip)^{0.03} OCR^{0.47}$	Norwegian clays, oedometer and K_0 triaxial tests	
8	$K_{0oc}= 0.57 OCR^{0.39}$	Brooker and Ireland dataset	
9	$K_{0oc}= 0.53 OCR^{0.47}$	Norwegian clays	
10	$K_{0oc}= 0.53 OCR^{0.53}$	Sands, high quartz	Narongsirikul et al., 2020
11	$K_{0oc}= 0.47 OCR^{0.47}$	Sands, low to medium quartz	
12	$K_0 = 0.034 V_{cl}+0.3681$	Synthetic Silt and clays	Grande et al 2011 and 2013
13	$I_p=0.9971 \cdot V_{smectite}+20.36$	Based on limited dataset	Grande et al 2022
14	$K_0=0.003 \cdot V_{smectite}+0.5343$	Based on limited dataset	
15	$K_0=((0.034 \cdot V_{cl}+0.3681)+(0.003 \cdot V_{smectite}))\cdot(OCR)^{0.47}$	Combined relationship (V_{cl}, $V_{smectite}$ and OCR) based on Eq. 13, 14 and 9.	

The multiple regression analyses performed by L'Heureux assumed an exponential form equation linking the coefficient of earth pressure at rest with the plasticity index and OCR. The general form of the equation was:

$$K_0=a\,I_{p^b}\,OCR^c \qquad \text{Equation 16}$$

where K_0 is the coefficient of earth pressure at rest, I_P is the plasticity index of the clay, and OCR is the overconsolidation ratio. The a, b and c parameters are empirical factors describing the best fit from the regression analyses.

This general term is also the basis for further work reported herein. We select them to further describe the two main contributing elements in the equation;

The first part of Equation ($a\,I_{p^b}$) defines the K_0 in the normally consolidated regime (K_{0_nc}, i.e. when assuming OCR=1). This part is sometimes referred to as a function or simplified with a constant (0.47, 0.53 or 0.57). L'Heureux found a limited impact of the plasticity index (I_p) for Norwegian quarternary clays where V_{cl} and I_p has limited variation due to high content of silt in glacial sediments. Then by using a constant value it can be useful to represent the average behaviour in the normally consolidated regime. However, for the mudstones and shales in the North sea, the first part of equation can be more relevant because higher content of clay and sometimes higher content of plastic clays like smectite (i.e. Oligocene and Eocene mudstones) than in Norwegian quarternary clay (Bjørlykke, 1998, Bjørslev Nielsen et al., 2015).

Second part of equation (OCR^c) defines the K_0 in the overconsolidated regime (K_{0_oc}, i.e. when assuming OCR>1), and where c is the exponent found equal to 0.47 in several studies. The more general term will then be

$$K_{0_{oc}} = K_{0_{nc}} \cdot OCR^c \qquad \text{Equation 17}$$

In the SHARP project we explore both K_{0-nc} and K_{0-oc} relation by including more datasets serving as input K_{0-nc} equations in Table 2-2. Among these are;

1. φ of remoulded material, for use in Eq.1 and 2
2. K_0 vs. $V_{smectite}$ for use in Eq.15
3. I_p vs. $V_{smectite}$ for use in Eq. 3-7
4. I_p vs. V_{cl} for use in Eq. 3-7

2.3 Laboratory testing at NGI

2.3.1 Analysis of tests from geotechnical and shale database

Data from geotechnical site investigations in Oseberg and Troll in the Horda Platform area have been analysed and compared with a larger dataset from the NGI database. The work focused on interpreted parameters obtained for standard Oedometer tests performed on clays and sands. Oedometer tests are uniaxial (1-D) consolidation tests performed understandardized procedures in NGI laboratory (Sandbækken et al., 1986). The parameters obtained are consolidation parameters, mainly constrained modulus (M) and permeability (k). Relations between deformation parameters and index parameters of Ip and volume of clay from sieve analysis (clay fraction < 0.002 um) have been investigated. Mineralogy data from XRD have been included when available. The synthetic silt-clay mixtures with well known mineralogy (Mondol et al., 2019, Grande et al. 2011, 2013 and 2022) are used for reference and the same dataset is also used for the calibration of the constitutive model in DV1.1 and DV1.2. The idea is to check how natural lithologies representative of the Horda platform fit within this framework empirical relationships and constitutive models to be used in stress history modelling in WP1.

The representative lithologies from the Troll area have been included as a reference dataset for shales for comparison with available data (WP3.2) and potential consolidation analysis to be performed under WP1.3 (see Appendix A- Mineralogy, deformation and permeability data from Horda platform. These are data released by Equinor and the relevant licences and data are resetricted for SHARP project until publication). A detailed documentation of Quarternary units is given in Lunne et al., (2006) and the SHARP report DV1.1a and also summarized in the NTNU master thesis (Jalali, 2022) .

2.3.2 New tests under SHARP- Drake shale

Reference geotechnical tests on crushed Drake shale material were done as part of WP3.2. This includes plastic and liquid limit (wP-wL) and plasticity index (Ip). Liquid limit method is determined by fall cone method with a 60 gr/60 degree cone using a one-point test. Column T will be ticked if the four-point liquid method is used. Test procedures are according to NS-EN ISO 17892-12:2018

The parameters of Drake shale are wP=20%, wl=33% and Ip=13.

The friction angle was measured based on Direct Shear Test (DST) on reconstituted Drake shale material after the same procedures as for the Draupne test performed preciously at NGI (Da Silva 2022). The sample is consolidated at normal stress of 1497 kPa and then sheared to maximum deformation of 10 mm (see Figure 2-1). The peak

shear stress is 726 kPa. From this, the calculated friction angle is 25.8°. This value is based on the assumption of zero cohesion representing initial state under sedimentation in a low energy environment, which should be representative for sedimentation conditions for shales like lower Drake (main seal) which is from shallow-marine environment prodelta to delta front (Thomson, 2022)). Also only one DST test is available for this study, however, previous results from several DST show limited impact on friction angle when using zero cohesion (tested on data from DaSilva, 2022). Friction angle is interpreted at peak failure of remoulded material. Direct Shear tests on remoulded material is the same as the reference friction angle for clays tested in the Brooker and Ireland, 1965 study.
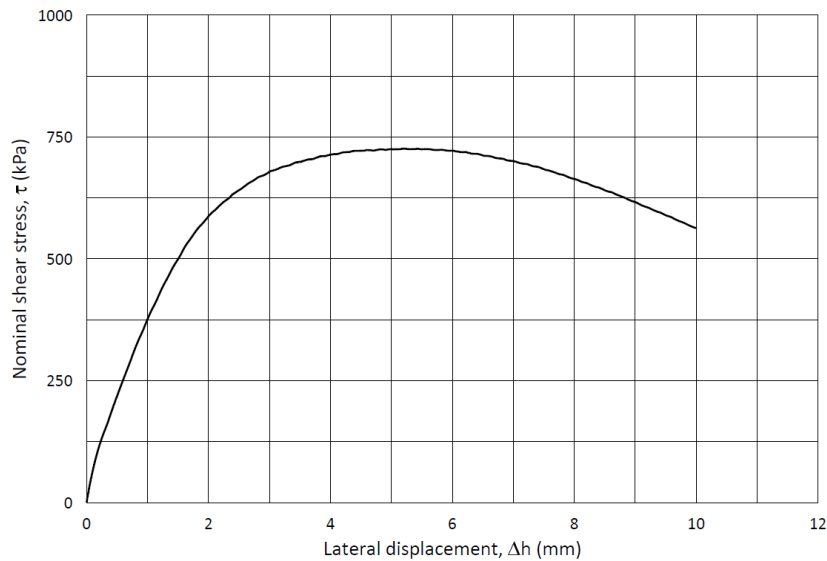

Figure 2-1 Results from direct shear test (DST) on Drake reconstituted material performed at NGI under SHARP project. Nominal shear stress vs. lateral displacement.

Drake shale is the sealing unit in the Aurora storage site. NGI has performed an extensive laboratory test program on the same core from Drake and cores from sandstones of the Cook and Johansen Fm. (Griffith et al., 2023, CO2 datashare). The crushed sample is the remaining pieces of host rock after drilling several plugs for the main test program.

Results are included in the next chapter for estimation of K_0 based on the friction angle of remoulded clay and the plasticity of the material.

2.4 K_0 vs. friction angle of soils

Jaky (1944) established a theoretical solution where K_0 was presented as a function of the effective friction angle (φ') of the soil with the following simplified expression that has been widely used;

$K_0=1-sin\varphi'$ (Equation 1, Table 2-2)

An examination of the Brooker and Ireland (1965) test results showed a form of an equation similar to that proposed by Jaky (1944):

$K_0=0.95-sin\varphi'$ (Equation 2, Table 2-2)

Using the friction angle measured from cemented rocks with a significant cohesion with these relationships will not reproduce representative K_0 values for sediments

experiencing a burial history involving cementation. However, when rock samples are crushed down to powder the friction angle representative of a sediment with the actual mineralogical composition can be tested. This method was applied for the Drake Shale (in section 2.3.2) which gave an effective friction angle of remoulded material of 26.8°. Brooker and Ireland in 1965, tested also their most plastic Bearpaw shale with 60% of Montmorrilonite (Smectite) in remoulded (crushed state) and effective friction angle of remoulded material is reported to be 15.5° (based on Peterson et al., 1960). The friction angle for reconstituted Draupne shale from Ling depression has also been measured in direct shear testing in NGI laboratory (Da Silva, 2021) showing effective friction angles of 18.8° -22.3°. This shale is analogous to the Draupne in the Smeaheia area in the North Sea and has been thoroughly tested and documented for geomemechanical parameters (i.e. Skurtveit et. al, 2015, Soldal et al., 2021) but also directly tested under uniaxial strain for K_0 (Zadeh et al., 2017)).

An expected range of K_0 based on friction angles from these studies and using Equation 2 (Brooker and Ireland, 1965) are shown in Figure 2-2 in comparison estimated K_0 based on reported friction angles of clays. There are several studies reporting the friction angle from mixtures of clay vs. mineralogy, and some examples are summarized in a study on frictional behaviour of faults gauge (Da Silva, 2021). The mineralogy of the clay within has strong impact on the frictional strength within a fault gauge as well as the K_0 during initial sedimentation. Ikari et al. (2009) tested clay-rich synthetic gouges under triaxial conditions with effective normal stresses of 12-59 MPa. The gouges used included a 50-50 mixture of montmorillonite and quartz, a powdered illite shale, and a powdered chlorite schist. The friction measurements yielded friction angles inferior to 19°, with the montmorillonite gouge having significantly lower friction (10.8°-13.1°) the illite- and chlorite-rich gouges (15.1°-17.7°). The expansive Al-Qatif clay used by Dafalla (2013), dominated by illite and smectite, shows distinctively higher friction angles (33.4°-38.7°). Mixtures of kaolinite and Ottawa sand tested by Simpson and Evans (2016) gave friction angles of in range 25-33.5°, where 100% kaolinite give lowest friction angle of 25°.
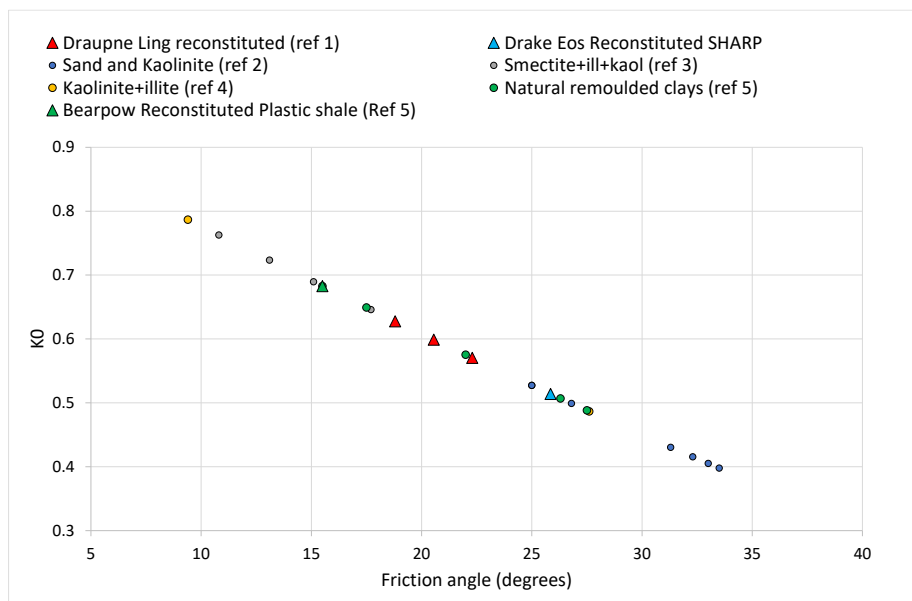

Figure 2-2 Calculated K_0 value vs. friction angles in reconstituted shales Drake from Eos Aurora and Draupne from Ling depression compared with synthetic clay mixtures, Da Silva (2021) [1], Simpson and Evans (2016) [2], Ikari et al. (2009) [3], , Dafalla (2013), Frikha and Jellali (2017) [4], Broker and Ireland (1965) [5]. The K_0 value is calculated according to equation $K_0=0.95-sin\varphi'$ from friction angle (Brooker and Ireland 1965). K_0 was not measured directly in this project.

2.5 K_0 vs. effective stress level

2.5.1 K_0 during loading and unloading

The K_0 vs. effective vertical stress for entire test and K_0 vs. OCR under unloading phase are shown in Figure 2-3a and b respectively. The dataset of synthetic clays and sand (Grande et al. 2011 and 2013), have been updated with natural clays, mudstone and shale. The natural quarternary representative also for sediments in Hordaplatform shows similar behaviour as the synthetic clays with quick stabilization at low effective stress and constant values of K_0 in range 0.55-0.58. For rocks it normally requires very high effective vertical stress for K_0 to stabilize at a constant value during loading. However, the mudstone and cemented shale show a clear drop in K_0 during loading, and the K_0 increases before almost stabilizing at K_0 of 0.6 and 0.4 respectively. Such stress drop is observed in several shales tested for industry, and the reported K_0 before stabilization can then be to low and cannot be used for simulating the K_0 at in-situ conditions.
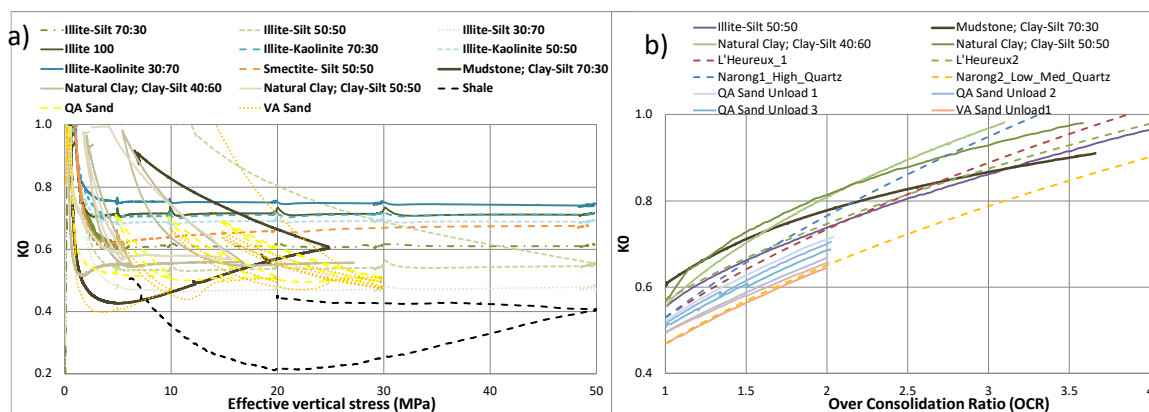

Figure 2-3 K0 vs. effective vertical stress (a) and K0 vs. Over consolidation ratio (OCR) (b) of silisiclastic sediments and rocks. Reference dataset of synthetic clays from Grande et al. 2013 are updated with example data from natural clays, mudstone and shale from NGI database.

The development of K_0 vs. OCR during the unloading (Figure 2-3 b) indicate a gradual increase of K_0 is observed for all tests where unloading cycles have been included. K_0 reaches close to 1, isotropic stress, at unloading corresponding to OCR of ca 3-4. For the sands there are three cycles of unloading and reloading, the development of K_0 during unloading is very similar and seems not to be sensitive to level of effective stress tested here (maximum effective stress 30MPa and OCR=2 in all cycles). The natural clays and mudstone shows a similar response with increasing K_0 during unload, however, for the shale sample the K_0 is almost constant during unloading. This is an important finding providing evidence that K_0 is increasing during drained unload also for normally consolidated mudstone down to at depth of ca 700 m. This is something that should be accounted for in stress prediction workflows and now implemented in SHARP modelling framework (see DV1.1 and DV1.3 report). The limit for this behaviour is not known however, the K_0 in the shale sample from 3.2 km, indicates that K_0 may be insensitive to unload below deeper than depth where cementation takes place (>2-2.5km, 70ºC). Berre 1996 reported a reduced value of K_0 during drained unloading from $K_0 = 0.58$ to $K_0 = 0.35$ at maximum unload. This demonstrates that K_0 may even reduce. Stiff uplifted shales from Barents sea have a trend with increasing K_0 during unload (Grande et., al 2011). However, those are older datasets were performed with less accuate instrumentation and those data may be re-checked.

2.6 K_0 vs. content of clay, smectite and plasticity index (Ip)

Relations between K_0 and the content of clay (V_{cl}), smectite (V_{sme}) and plasticity index (I_p) were evaluated and presented in Grande et. al 2022 as part of SHARP project. These are listed in Table 2-2, Eq.13,14 and 15. Also, relations between smectite and Ip have been tested to give a more useful correlation for deeper lithologies where plasticity index is not well known. All these relations have been further evaluated with more datasets of clays, sands, mudstones and shale in Figure 2-4. The new data confirms the earlier documented trends, however, K_0 data for shale tests that has not been stabilized deviates as expected with lower values of K_0.
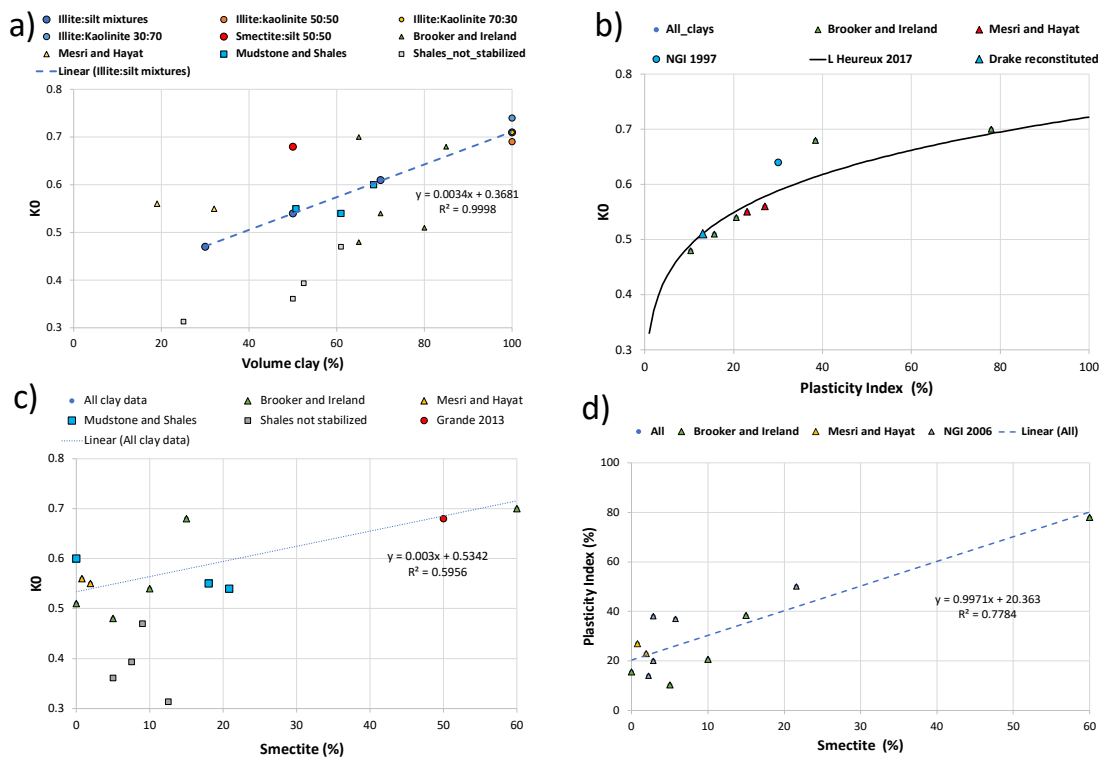

Figure 2-4 Correlation charts for K0 vs. volume clay (a), plasticity index (b), volume smectite (c) and plasticity index vs. volume smectite (d). Original figures from Grande et. al., 2022 based on synthetic and natural clays are updated with data from mudstones and shales from database and test on reconstituted Draupne shale.

The Ip vs. V_{cl} relations were investigated from the geotechnical dataset from Troll and Oseberg (plot in Appendix A), and the following new correlation equation for Ip vs. V_{cl} were established based on a large geotechnical dataset;

$$I_p = 0.7995 \cdot V_{cl} \qquad \text{(Equation 18, All data)}$$

Where I_p can be applied into general correlation from L'Heurex 2017;

$$K_0 = 0.33 \cdot I_p^{0.17} \cdot OCR^{0.39} \qquad \text{(Equation 4, Table 2-2)}$$

From relations in the figures above it is possible to apply relationships in different ways: K_0 from content of V_{cl}, I_p, or volume mectite directly, or through relating smectite or V_{cl} to I_p and then K_0 from I_p from standard geotechnical relationships. Note, the datasets are inter-related to some extent, with both V_{cl} and smectite content contributing to K_0

meaning that a real separation of effects is not possible with this dataset. The methodologies are demonstrated in Chapter 6, in SHARP DV1.2 report and in Grande et al 2022.

2.7 Constrained modulus of clay, mudstone and shales

Relations between constrained modulus and permeabilities of clays, mudstones and shales were investigated. While these are not the main focus, it provides useful input to consolidation modelling and evaluation of load vs. time and drained vs. undrained behaviour of clays and shales. The modulus and permeability relationships are important input to consolidation modelling to evaluate stress history from glacial loading within quarternary units (NTNU work) and the uplifted overconsolidated units below (work under WP1.3). Input parameters and resulting data plots are document in Appendix A.

2.7.1 Consolidation behaviour vs. effective stress

In this section we evaluate the constraind moduls M vs. effective stress, and together with the permeability k (next section), M is a key parameter in the modelling of consolidation of clays undergoing uniaxial compaction. These parameters are input in modelling of changes in stiffness under burial history of sediments and can be applied as input in stress history modelling in SHARP WP1. The relation between modulus (M_o) and modulus number (m) and index properties clay fraction (V_{cl}), plasticity index (Ip) and water contents (wi) have been investigated from the geotechnical data from oedometer tests from Troll and Oseberg.

One dimensional deformation in the oedometer can be represented by the Janbu model (Janbu 1969). and the definition of the Janbu parameters are shown in Figure 2-5. Tangent modulus (or constrained modulus), M, is the ratio of the change in effective stress $(\Delta\sigma')$ to the change in strain $(\Delta\epsilon)$ for a particular load increment (i.e. $M = \Delta\sigma') '/ \Delta\epsilon)$. For natural clays and at low-stress level, around σ'_{v0}, the modulus (M_0) is large due to effect of overconsolidation of sediment. When σ_v' increases, the modulus decreases owing to partial collapse of the grain skeleton and modulus reaches a minimum around p_c'. Subsequently, when σ_v' is increased beyond pre-consolidation stress (p_c'), modulus increases linearly with increasing σ_v' in the normal consolidation stress range and modulus $M = m (\sigma_v'-\sigma_r')$ where m is the modulus number and σ_r' is the intercept of m on the σ_v' axis and it called the reference stress (for $\sigma_v' > p_c'$). Janbu method and identification of p_c' and is also one of most common method to define the maxim pre-consolidation stress previously experienced in sediment in the nature.
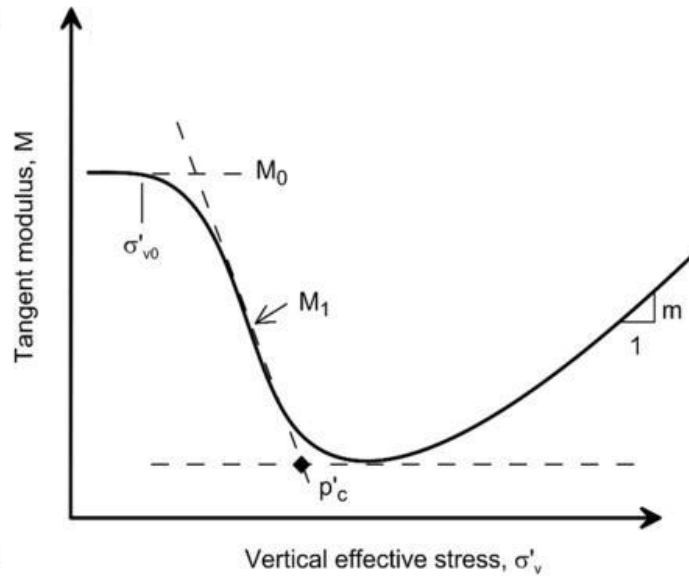
Figure 2-5 Illustration of Janbu model and Janbu parameters describing the tangential modulus M vs. effective vertical stress (figure from Lunne et al. 2008).

2.7.2 Constrained modulus vs. index properties

The relation between modulus (M_o) and modulus number (m) and index properties clay fraction (V_{cl}), plasticity index (Ip) and water contents (wi) have been investigated from the geotechnical data from oedometer tests from Troll and Oseberg. M_o was poorly related to index properties although when normalizing for p_o' and p_c' and relations are therefore not reported here. However, although some scatter in the datasets, the correlation between m and index parameters (i.e., V_{cl}, Ip, Wi) is rather clear (Appendix A) and the equations are reported below (Eq.1, Eq.2. The correlation with V_{cl} may be useful in combination with information from the clay-rich sediment in the various lithologies. Ip and Wi are typical parameters for geotechnical site investigations and can be useful to assess the modulus numbers. The use of modulus numbers should be limited to depth range where only mechanical compaction is expected.

$$m = -0.2816 \cdot v_{clay} + 28.52 \qquad \text{Equation 19}$$
$$m = -0.1418 \cdot \ln(I_p) + 64.79 \qquad \text{Equation 20}$$
$$m = -11.77 \cdot \ln(w_i) + 60.261 \qquad \text{Equation 21}$$

2.7.3 Constrained modulus vs. pre-consolidation stress

The established relation between modulus number (m) volume clay (V_{cl}) (Eq.19) is used to calculate constrained modulus M for some representative lithologies in the Horda area: Lista, Draupne and Drake (from Appendix A) and compared with the synthetic silt and illite mixtures from NGI database in Figure 2-6a. Also, a comparison of M based on modulus numbers from clay content derived for Lista, Shetland, Draupne and Drake shales and the actual M value determined in rock mechanical testing (Appendix A) are shown in Figure 2-6b.
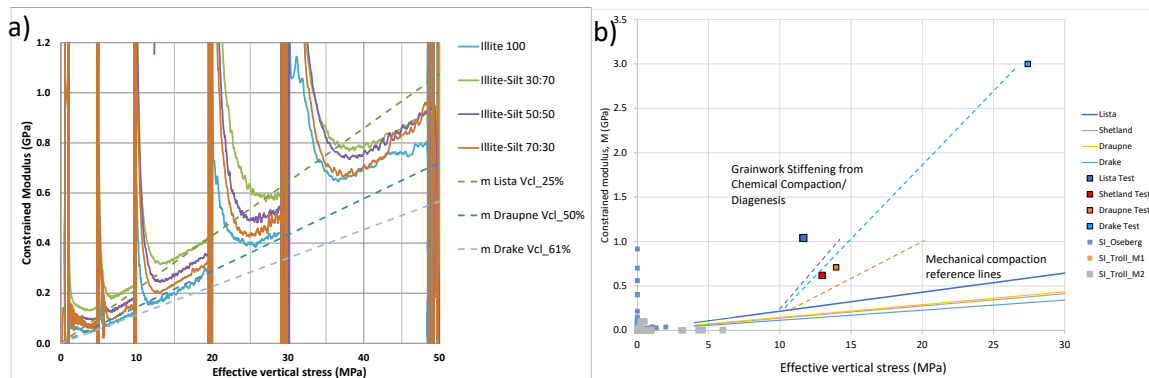
Figure 2-6 a) Tangential constrained modulus vs effective stress in synthetic and natural clays and mudrocks (updated plot based on Grande et al. 2013). b) Constrained modulus vs. pre-consolidation stress from rock mechanical tests compared with trendlines based on geotechnical database Horda platform. The dashed lines are only indicative for grain framework stiffening from effective vertical stress of 10 MPa corresponding to maximum burial depth of 2 km. Diagenetic effects are considered within WP1 (see discussions in DV1.1b, DV1.2 and results in DV1.3 reports).

The estimated values of tangential modulus vs. effective stress based on clay content in Lista, Draupne and Drake are in the same range as for the syntetic clay mixtures data in Figure 2-6a. Figure 2-6b shows the actual difference expected between the mechanically compacted clays and the actual chemically consolidated shales Lista, Shetland and Draupne and Drake. The plot indicates the hugh impact of cementation on grain stiffening. The use of the given m vs. V_{cl} relationships for clays is valid only for the subsurface shallower than certain depths ca 2-2.5km (temperature <70°C), where mechanical compaction is the governing process. Beyond these depths diagenetic processes, cementation, and changes in mineralogy become more significant, leading to a shift in the governing mechanisms. In such cases, alternative methods and parameters should be considered for characterizing the subsurface. For discussion of constitutive relationships also incoorprating effect of diagenesis, see SHARP report DV1.1b and DV1.2, also referring to Prats et al., 2019, Wangen et.al 2000 and Roberts et. al 2014).

Correlation between modulus number (m) and volume clay (V_{cl}), Plasticity index (I_p) and water content (w_i) can be used to address the expected constrained modulus within the mechanical compaction regime. All parameters V_{cl}, I_p and w_i can be useful for geotechnical applications where such information are typically available. For deeper applications V_{cl} may be more useful correlation parameter. The reference shales from the Horda platform are chemically compacted with significantly higher constrained modulus.

2.8   Permeability of clays, mudstones and shales

In this section we evaluate the permeability k vs. effective stress, which together with M, is a key parameter in the modelling of consolidation of clays undergoing uniaxial compaction. These parameters are input in modelling of changes in stiffness during burial history of sediments and can be applied as input in stress history modelling in SHARP WP1. Published trends of permeability vs. effective stress and porosity for various compositions of mechanically compacted synthetic mudrocks are presented in Figure 2-7a and Figure 2-7b (from Mondol 2009, and 2011). The results show a systematic reduction in permeability vs. effective stress and porosity reduction when increasing clay content in mixtures of kaolinite vs. silt and illite vs. silt. The influence

of mineralogy on permeability and permeability anisotropy vs. porosity reduction, show that mixture with 50% smectite and 50% silt has the lowest permeability, even lower than all the 100% clay mixtures of various fractions of illite and kaolinite. The permeability is less influenced by the reletaive amount of illite vs. kaolinite in this case.
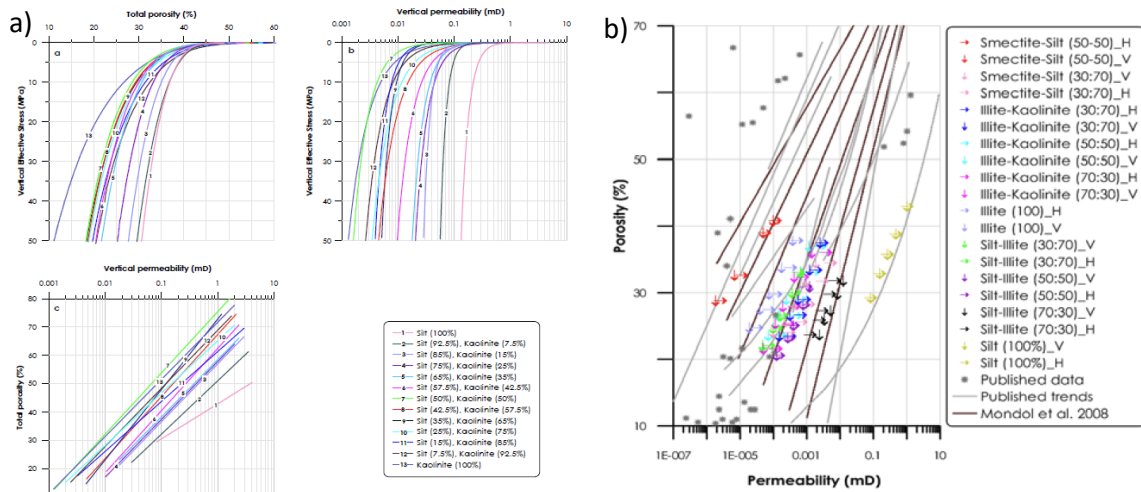

Figure 2-7 a) Permeability (Mondol et.al 2009). Cross-plots of (a) total porosity and (b) vertical permeability versus vertical effective stress of mechanically compacted brine-saturated silt-kaolinite mixtures. Another cross-plot of porosity and permeability (c) found for same brine-saturated synthetic mudstones. The x-axis representing permeability is plotted in a logarithmic scale (b and c). Permeability anisotropy (Mondol et.al 2011). A comparison of published porosity permeability relations of a series of natural mudstone, uniaxially compacted remoulded mudstones (Mondol et al. 2008) and triaxially compacted 10 synthetic mudstones

Permeabilities of shales from constant head permeability testing in triaxial cell from several fields in depth range 1-5 km has been summarized previously (Grande et. al 2019). This same dataset has been utilized here to compare permabilities from chemically compacted shales with those from mechanically compacted synthetic clays, natural clays and mudstones in the Figure 2-8a and Figure 2-8b. The reference shales from Nordland, Lista, Shetland , Draupne and Drake are highlighted (permeability tabulated in Appendix A). Permeability data from Troll and Oseberg oedometer tests are also included in the plots. For oedometer tests the permeability values are extrapolated to zero effective stress from k-line (Sanbækken et.al 1985). This is assumed to be the same permeability as for the in-situ state of sediment at the sample depth. The same assumption applies for normally consolidated conditions or if the sediments are overconsolidated due to ice-loading. In this case for Troll and Oseberg the permeability will represent the overconsolidated state of the sediment.
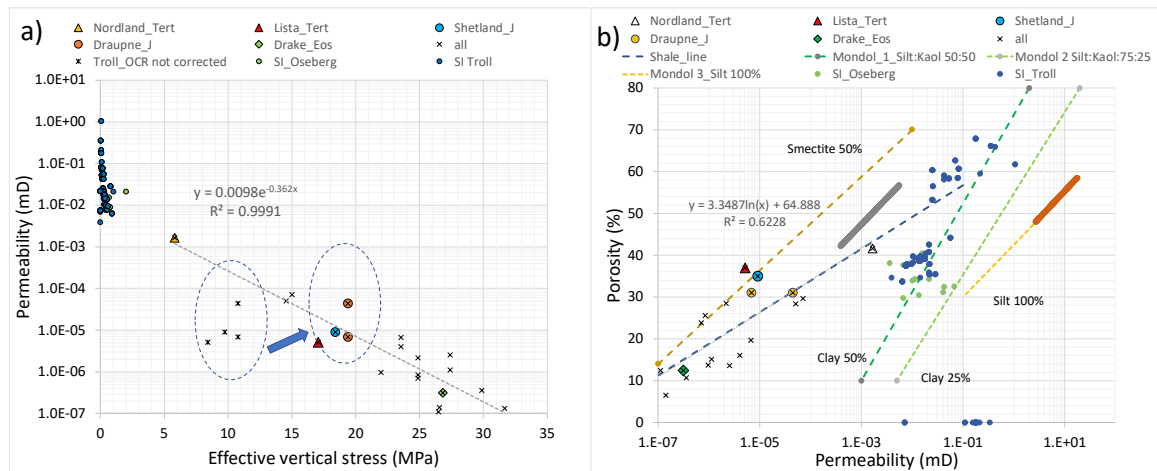
Figure 2-8 a)Permeability vs. effective vertical stress in natural clays, mudrocks and shales. b)Permeability vs. porosity in synthetic clays, natural clays, mudrocks and shales.

For the rock samples permeabilities from shales are in the order 1E-3 to 1E-7 mD, and varies based on porosities, water content, mineralogy, depth, effective stress during test and orientation of plug. The resulting correlation equations for permeability (k) and porosity (φ) from plots are ;

$$k = 0.0098 \cdot e^{-0.362 \cdot \sigma'_v} \qquad \text{Equation 22}$$

$$\varphi = 3.3487 \cdot ln(k) + 64.888 \qquad \text{Equation 23}$$

There is good agreement between the permeability of natural clays from soil investigation and the synthetic trendlines based on systematic studies (Mondol et al., 2009 and 2011). The smectite-rich sediments have the lowest permeability trend vs. effective stress and the silt-rich sediments have highest permeability trend. The permeability vs. maximum pre-consolidation stress of the chemically compacted mudstones and shales can be simplified using a linear trendline, and give a much better corelation compared to permeability vs. present-day stress (i.e. not corrected for uplift).

3 Triaxial K_0 testing and modelling of stress history in Quaternary units

3.1 Introduction and background

NTNU efforts focus on geotechnical profile of Troll, which is well studied and documented through Troll soil investigation reports available under SHARP and in literature (i.e. Lunne et al., 2006). Part of the work related to glacial history and impact on stress and rheology of quaternary sediments are aligned with both WP1 and WP3, and similar works are also reported in DV1.1a, DV1.1b and DV1.2. The consolidation analysis performed within the quaternary to simulate the impact of stress history on the present day in-situ stress and mechanical behaviour of quaternary sediments. Three Master Thesis works documents the detail of this work, and Master Thesis documents are available for SHARP and public after officially approved.

Triaxial K_0 testing is performed as part of master thesis study at NTNU. Two well-preserved cores with soft clay from Onsøy test site in Halden, Norway, were sent to NTNU Laboratory. Previously they were storage at NGI after being sampled during another field campaign. The cores are from the depth interval of 6-8 m. This is the same depth as in-situ fracture tests performed as part of a previous project (Gundersen et al., 2019). Testprogram were designed in collaboration with NGI. NGI has also provided triaxial and oedmeter data from Troll soil investigation report for the numerical modelling work and contributing with relevant papers for geotechnical and geological background data for the study.

3.1.1 Short summary of offshore stress tests and Onsøy onshore test site with hydraulic fracturing experiments

The Onsøy soft clay test site has been extensively investigated first Onsøy since 1968. In 2016, the Norwegian Geotechnical Test Site (NGT) project established five research sites, one of which is the NGTS Onsøy soft clay site. The lightly overconsolidated soft clay site has been characterized based on extensive *in situ* and laboratory testing. *In situ* methods include electrical resistivity tomography, multichannel analysis of surface waves, total soundings, rotary pressure soundings, cone penetration testing with and without seismic and electrical resistivity measurements, dilatometer with seismic measurements, self-boring pressuremeter, electric piezometers, thermistor string, hydraulic fracture testing and earth pressure cells (Gundersen et al., 2019). The Onsøy clay was deposited after the last glaciation as a marine clay and it is very similar to several clay deposits found at oil and gas fields offshore Norway, i.e Troll field and Luva (later name changed to Aasta Hansteen) field.

Figure 3-1 illustrates the similarities between Luva, Troll and Onsøy historic sites in terms of plasticity index (I_p) and OCR. The measured Ip in tested cores and the simulated final OCR from unloading phase of NTNU K_0 tests are indicated.
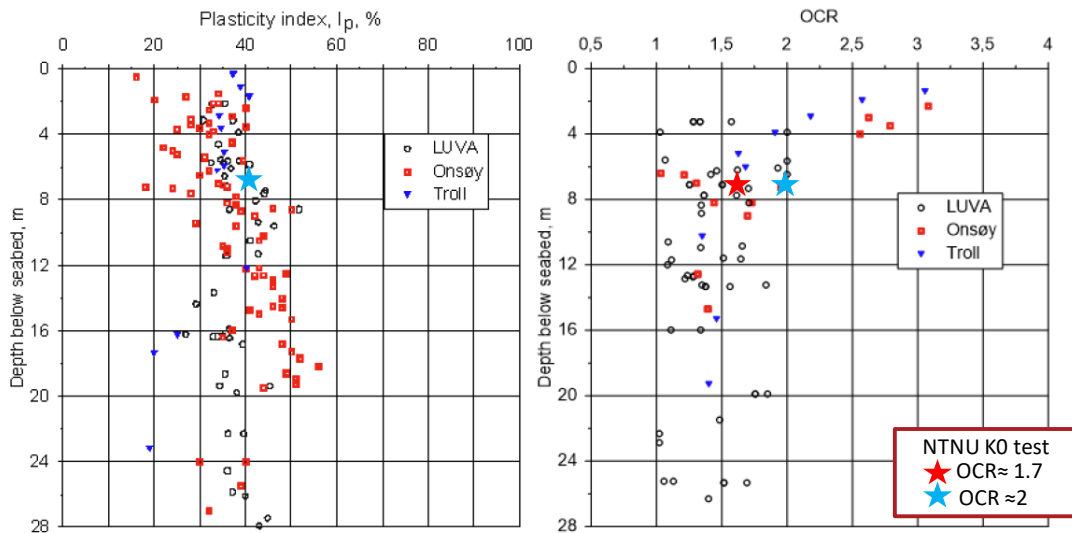
Figure 3-1 Plasticity index and over consolidation ratio with depth for the offshore sites Luva and Troll, and the Onsøy historic site (Gundersen et.al 2019). The plot is updated with measured Plasticity index and simulated OCR in the NTNU test program from Myhrvold and Kopperud (2023)

3.2   Master thesis work

3.2.1   Master Thesis by Jalali 2022

The title of thesis is "Consolidation and stress history in shallow sediments in the northern North Sea". The thesis was submitted in December 2022, and is available at SHARP Teams site from Q2 2023. A short summary is given below.

Definitions of the relevant geotechnical parameters and the relationship between these parameters and stress history has been addressed through a literature study. In the next step, via the data sets provided by NGI and literature available, geological and geotechnical characteristics of the Troll field in the Horda platform have been studied, and accordingly, a simple model regarding layering, the chronology of ice-loading and the mentioned parameters are proposed. In the end, a two-dimensional numerical model has been generated in PLAXIS and through a calibration process, the laboratory test results have been simulated. The procedure of Soft Soil Creep (SSC) modelling by PLAXIS was adopted.

Results from model indicate that K_0 from model (range ca 0.47-0.95) fits reasonable for most layers, exception the highly over consolidated Unit III where a K_0 of 0.8 and 1.2 was obtained from model and empirical correlation respectively. It is suggested in further work to use an advanced creep model that implements the concept of kinematic hardening. Since in this problem, the behaviour of soil in terms of millions of years is intended, creep phenomena have a substantial role and the development of K_0 influenced by creep is not satisfactorily clear (i.e. Grimstad et al. 2021). As a next step it was suggested to use the models that implement the kinematic hardening concept (i.e. Davood et al., 2022)

3.2.2 Master Thesis by Tubid Myhrvold and Valle Kopperud 2023

Thesis is named "Consolidation and Stress History in Shallow Sediments in the Northern North Sea" is a cooperation between two students, Jan Alexander Tubid Myhrvold and Alf Erik Valle Kopperud (Myhrvold and Kopperud, 2023). It is an extension of the work performed by Jalali (2022), and was building on previous PLAXIS model, loading scenarios and geological and geotechnical framework developed earlier. Two cylinders from Onsøy (Troll analogue) from depth interval 6-8 m were tested by students at NTNU laboratory. The tests cores had similar index properties similar to previous tests from Onsøy (seeFigure 3-1 and Figure 3-2). Four K_0 tests were done with unloading and reloading cycles to simulate the stress at Onsøy for calibration with in-situ field stress tests, and furthermore, loading and unloading cycles at higher stress were done to similate glacial loading and unloading in the Quarternary units in Horda platform. Results from the four tests are shown in Figure 3-3. The results are compared in the Onsøy and Troll test site in Figure 3-4 and Figure 3-5. Earlier PLAXIS modelling work used the soft soil creep model (SSC) was now extended by including the kinematic hardening concept in a Hyper-Viscoplastic Modified Cam Clay model (HVMCC, i.e. Davood et al., 2022). The two models are compared for borehole 8903 Unit III in Figure 3-5 showing that HVMCC model give higher an more realistic values of K_0 (closer to 1) compared to the SSC model (K_0 ca 0.8).
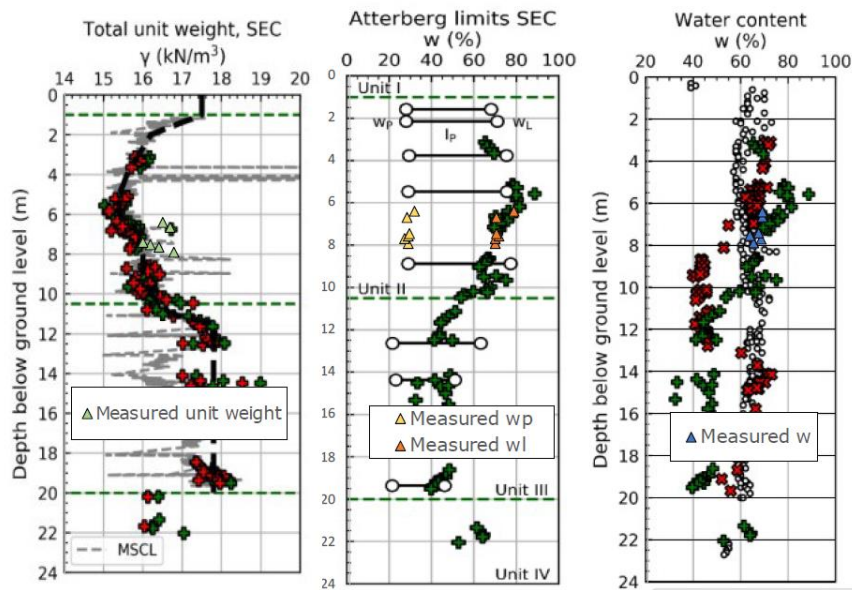

Figure 3-2 Comparison of index parameters, total unit weight, Atterberg limits and water content based on measurements from Onsøy test site (Gundersen et al., 2019) and clay interval 6-8 m tested in master thesis (Myhrvold & Kopperud, 2023).
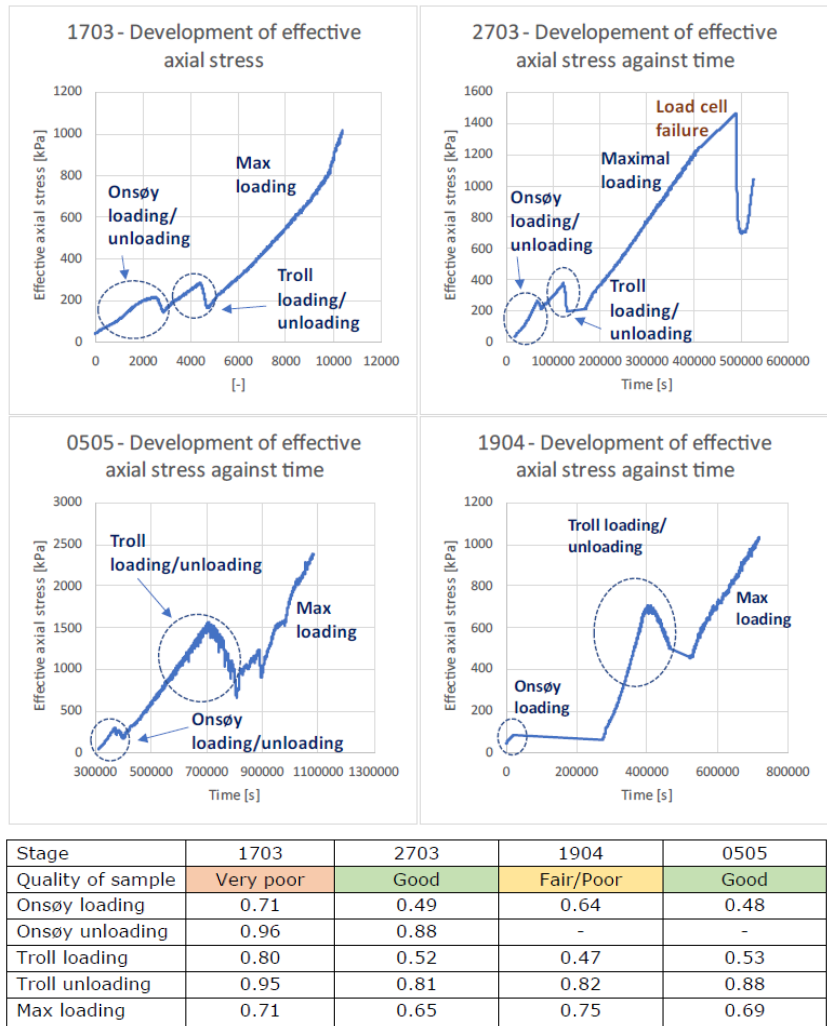
Stage	1703	2703	1904	0505
Quality of sample	Very poor	Good	Fair/Poor	Good
Onsøy loading	0.71	0.49	0.64	0.48
Onsøy unloading	0.96	0.88	-	-
Troll loading	0.80	0.52	0.47	0.53
Troll unloading	0.95	0.81	0.82	0.88
Max loading	0.71	0.65	0.75	0.69

Figure 3-3 Effective axial stress vs. time development in four triaxial K_0 tests (1703, 2703, 1904 and 0505) and summary of assessed K_0 values. The test simulates the load history in the Onsøy test site and Troll. Figure and tabulated results from Master Thesis (Myhrvold and Kopperud, 2023).

3.3   Comments to Master thesis results

We comment here briefly on results and for SHARP reporting and independent on the discussion in Master Thesis work. For detailed discussions and comments by master students we refer to Jalali (2022) and Valle Kopperud and Tubid Myhrvold (2023).

The index parameters of tested Onsøy clay total unit weight of 16-17kN/m^3 and water content 63-69% and I_p of 41.6-43.1% are in line with other samples in Onsøy from similar depth (see Figure 3-1 and Figure 3-2). When comparing to Troll profil these Onsøy samples are most representative of Troll I (0-16 m) and Unit IV (135-187) m plastic clay units with I_p of 37% and 34-39% respectively. Recommended in-situ values of OCR and K_0 are as shown for reference in Figure 3-5 are as follows; Unit 1- OCR of 1.45 and K_0 of 0.67 and for Unit IV- OCR of 2.35 to 2.55 and K_0 of 0.8 to 0.9 (values from Lunne et al., 2006).

Figure 3-4 illustrates the estimated K_0, and the *in situ* horizontal effective and total stresses with depth in Onsøy tests site as determined from various field tests and empirical relations, where the results from NTNU K_0 tests are included for comparison.
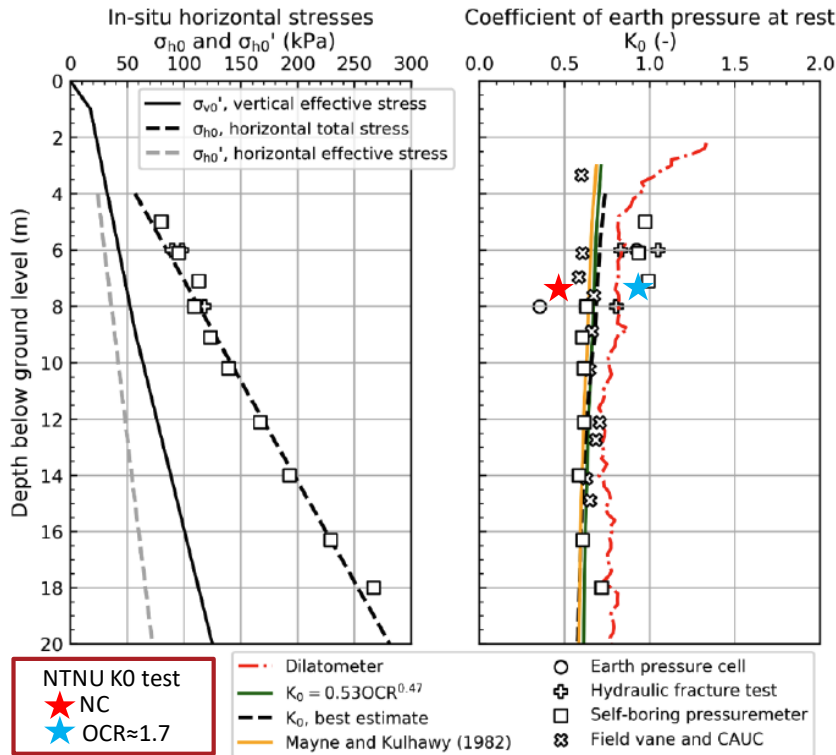
Figure 3-4 In situ horizontal effective and total stress and coefficient of earth pressure at rest, K0, with depth at Onsøy. Figure from Gundersen et al., 2019, updated with experimental results from NTNU K_0 tests (Myhrvold & Kopperud (2023). The K_0 tests is shown for normally consolidated (NC) and overconsolidated (OCR≈2) state.
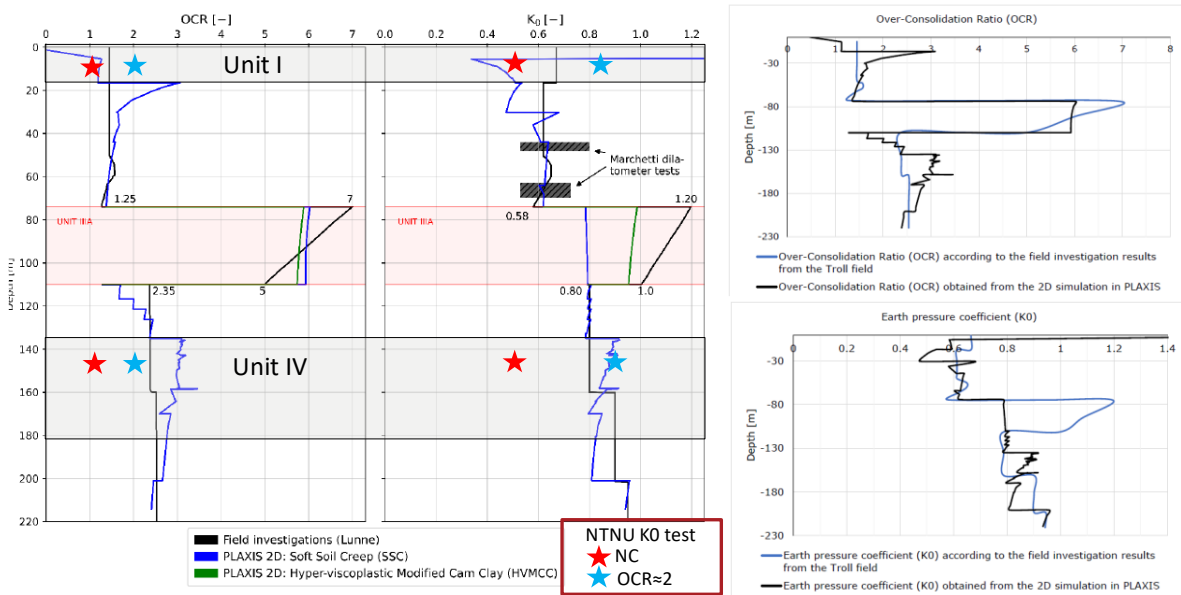

Figure 3-5 Present day OCR and K0 profile from simulation of stress history in the Quaternary units at the location of Troll East geotechnical borehole 8903. Figure from Master theis, updated with experimental results from NTNU K_0 tests (Myhrvold & Kopperud (2023). The K_0 tests is shown for ormally consolidated (NC) and overconsolidated (OCR≈2) state. Right plots show OCR and K0 profiles from Jalali (2022) for comparison.

We comment here briefly on the results from the two good quality tests (2703 and 0505) and compare to predictions from empirical relations (Eq.4, Table 2-2) based on the measured I_p of 41.6-43.1%. For Onsøy and Troll loading phase, the reported range of K_0

(0.48-0.53) is well in line with typical values for normally consolidated Norwegian clays but lower than predicted from Eq.4 ($K_{0\_nc} \approx 0.62-0.63$) which accounts for the relative high plasticity. The K_0 of 0.88 derived from Onsøy unloading phase (up to OCR≈1.71) is higher than predicted from Eq.4 but in range of K_0 from Onsøy field measurements (see Figure 3-4 depth interval 6-8m). The range of K_0 (0.81-0.88) from Troll unloading phase (up to OCR≈2) is close to the predicted from Eq.4 (K_0=0.82), and in range of recommended values (0.8-0.9) of Troll Unit IV, although the OCR applied in test is slightly lower comapared to in-situ OCR (OCR=2.35-2.55 in Unit IV) (see Figure 3-5).

Note that K_0 testing is not straight forward and the equipment and methods applied in NTNU laboratory deviates from NGI procedures. Also the interpretation procedure for K_0 used during unloading, is based on the secant method over larger interval rather than tangential values. This was due to unexpected behaviour of K_0 vs. effective stress behaviour likely due to experimental artefacts under unloading phase (i.e. swelling affecting axial stress). Also, there was a limitation of maximum stress in the equipement and the planned phases at maximum stress with larger unloading and OCR were not sucssessful in any tests. The K_0 from unloading in these experiments are therefore less reliable compared to K_0 from loading phase. Nevertheless, the K_0 in first and second unloading were found to be similar ($K_0 \approx 0.82-0.88$), which is expected after applying a similar OCR from a normally consolidated state.

Result for HVMCC model for Troll Unit III is shown in Figure 3-5, give larger values of K_0 ($K_0 \approx 1$) compared to the SSC model ($K_0 \approx 0.8$). Both values are lower than recommended K_0 of 1.2 in Unit III. For Cam Clay framework it has been demonstrated analytically that uniaxial loading gives $K_0 \leq 1$ and for the HVMCC numerical model K_0 was found to stabilize around 1+/-0.01 (Myhrvold and Kopperud, 2023). In cases of large unloading giving high OCR in uniaxial conditions, these numerical approaches cannot mimic results from previous laboratory studies and corresponding empirical correlations (i.e. Brooker en Ireland, L'Heureux et. al., 2017, Grande et al., 2011 and 2013).

A robust verification of K_0>1 from field tests is difficult, i.e. when using the most reliable hydraulic fracturing method (XLOT or Minifrac), the fracture opening will not exceed the least principal stress which for K_0>1 is the vertical stress. The field verification example at Onsøy have in-situ K_0 in range 0.8-1.1 (Figure 3-4), however, it was believed that water pressures were not maintained sufficiently long to minimize the effect of the disturbed zone to obtain the closure stress. This is also the typical situation for LOT tests in oil and gas wells. Other in-situ methods in Onsøy like self boring pressure meter and earth pressure cell give similar high values with K_0 in range 0.9-1, while field vane and CAUC give lower K_0 in line with empirical methods (Figure 3-4). In Troll well, Marchetti Dilatometer field test un Unit II indicates values of K_0 in range 0.5-0.8 (see Figure 3-5). Experiences from offshore North Sea tests are summarized in NGI 1990, and approximately 10 test are from Troll during site investigations (taking place in 1987, 1988, 1989) using Fugro McClelland Packer system as well as the Marchetti Dilatometer test shown in Figure 3-5 (from Lunne et al., 2006).

4 Assessment of permeability from stress cycling

Previous experiments conducted at BGS on pressure cycling in sandstone showed a strong hysteresis in porosity. The aim of this work is to examine the evolution of porosity and permeability for reservoir sandstone and clay-rich caprock. Two types of experiments have been proposed to look at the influence of stress history over geological time-scales and also during engineering operations, including depletion and inflation.

4.1 Methodology

The pore pressure oscillation apparatus (PPO; Figure 4-1) is a modified isotropic apparatus, as used at the Transport Properties Research Laboratory for over 30 years . The rig comprises of the following components:

Figure 4-1 The pore pressure oscillation apparatus

- A pressure vessel rated to 70 MPa.
- A modified vessel lid that allows the use of a flat-faced pressure vessel in order to minimise the downstream volume of the system.
- A lower sample platen, which has a porous disc in direct contact with the sample.
- A Teledyne/ISCO syringe pump to control the confining pressure of the test.
- A Teledyne/ISCO syringe pump to control the injection pore pressure of the test.
- Secondary pore pressure transducers on the injection, back-pressure and confining systems.

- Circuitry for full draining of all systems.
- Two logging systems using National Instruments cRio.

Each Teledyne/ISCO syringe pump was operated from a separate control box. This meant that the oscillating pore pressure could be generated by the controller using the Program function. Confining pressure could also be programmed to change, meaning that once started the operator only had to monitor that the test was not leaking and that each syringe pump had sufficient pore fluid.

The syringe pumps, two pore pressure sensors, and environmental parameters were logged using the main laboratory logging system, which could achieve records of approximately 10 seconds (0.1Hz). This interval is not sufficient for high permeability testing and so a second, dedicated, logging system was added to log three pore pressure sensors at a rate of 0.5 seconds (2Hz). It is not possible to log the same sensors on two logging systems and this meant duplicate sensors had to be added to allow "fast" and "slow" logging.

The sample was placed between the lower (injection) platen and the modified vessel lid (back-pressure) and was jacketed using heat-shrink Teflon. A robust jacketing arrangement has evolved at the BGS using lock-rings that ensure a secure barrier between the sample and the confining fluid. However, Teflon has a limited ability to stretch and this can result in jacket failure.
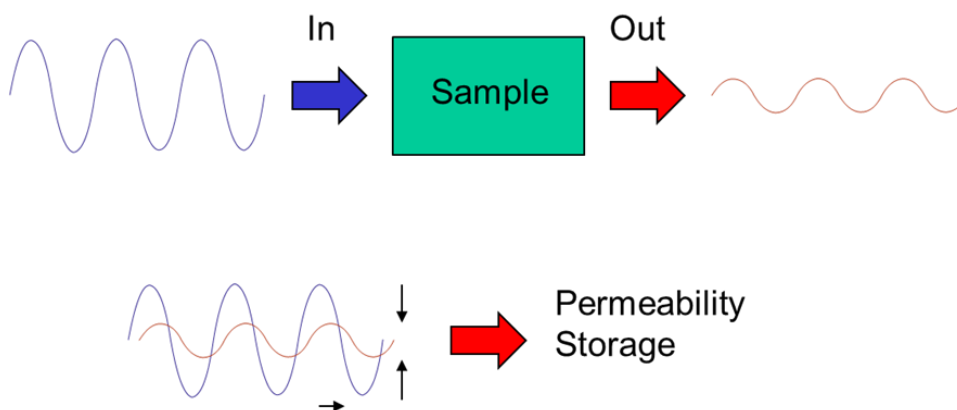

Figure 4-2 Rationale of the pore pressure oscillation technique

The pore pressure oscillation technique was proposed by Kranz et al. (1990) and Fischer & Paterson (1992). In this method a sinusoidally varying pressure is generated in the injection reservoir by means of a Teledyne/ISCO syringe pump. The pressure wave is transferred through the sample, where it is observed at the back-pressure end of the sample. This output wave is attenuated and has a phase shift as a result of the permeability of the sample. By analysing the input and output signals it is possible to calculate permeability and storage of the sample if the apparatus is calibrated well. Figure 4-2 shows the basis of the method. In order to calculate permeability the method described by Faulkner & Rutter (2000) was adopted.

Calculation of storage can be accompanied by errors, especially if the sinusoidal input is not optimised for the permeability of the sample being tested. However, the injection syringe pump recorded pore volume to a resolution of one micro litre. In generating an

oscillating pore pressure the volume of the pump was continually varying. However, filtering of the data gives average volume during a sinusoid and therefore offers a direct measure of changes of effective porosity. It has to be assumed that the pump has no leakage. Prior to testing the syringe pump is leak tested and only a leak rate of less than 1 μl/h is accepted.

Prior to testing the sample was assembled and carefully lowered into the pressure vessel. The confining vessel was filled and pressurised to 500 kPa. This should make all residual air go into solution. Once 500 kPa was established the pore pressure in the sample was carefully raised to 250 kPa. Using a system of valves and drains, the sample, filters and tube work of apparatus were flushed of air to ensure that the sample was fully saturated with pore fluid. The confining and pore pressure pumps were brought up to the starting pressures of 4 MPa and 2 MPa respectively in 500/250 kPa steps. The experiment was then started.
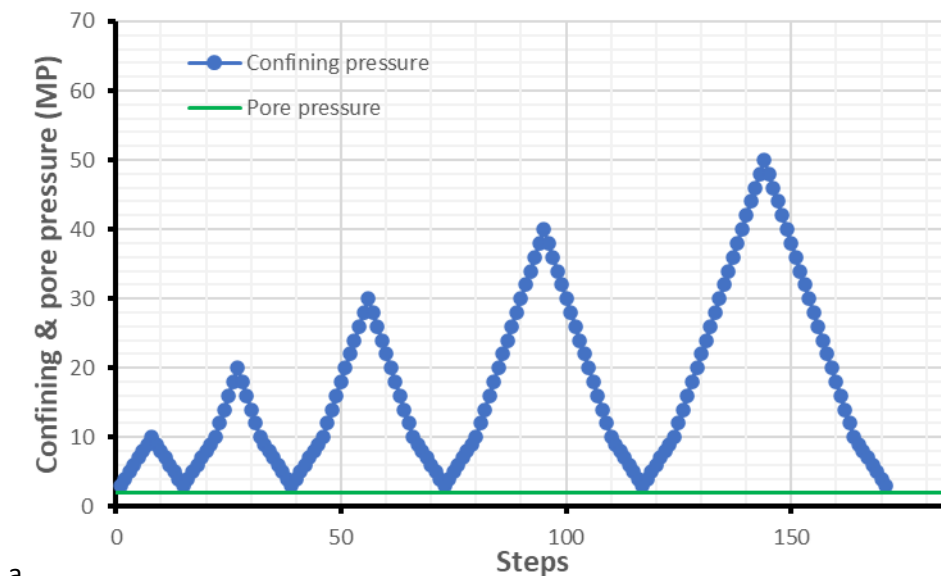
a
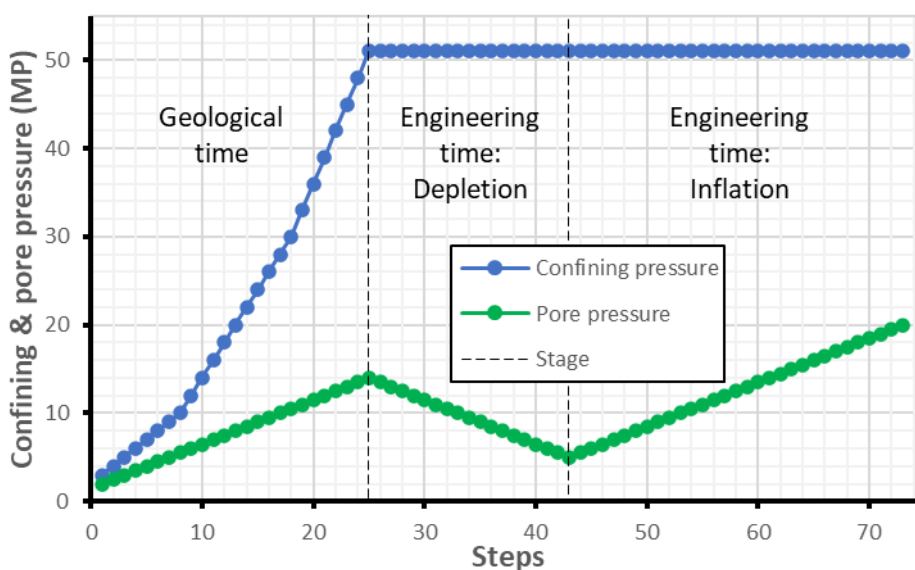
b

Figure 4-3 Boundary conditions of the test programme. Note the confining pressure and pore pressure shown in figure (b) will be defined from other work packages within Sharp to be relevant.

4.2   Experimental boundary conditions

Two different types of tests will be conducted. In the first (Figure 4-3a), pore pressure is kept constant with an average of 2 MPa (oscillating between 1 and 3 MPa). Confining pressure is then increased/decreased on cycles to 10, 20, 30, 40, and 50 MPa. It was hoped to operate to a maximum of 70 MPa, but this was not possible because of pressure limitations of the available syringe pumps. This test directly investigated stress history on permeability and porosity. The second type of test (Figure 4-3b) aimed to look at realistic history. In the first phase of testing confining and pore pressure will be increased to simulate a geological history of simple deposition. Confining pressure will then be fixed for the duration of the test. The next stage of investigation is designed to investigate the influence of depletion of pore pressure on permeability and porosity by reducing pore pressure. This will increase effective stress acting on the sample. The third, and final, phase of testing then simulates inflation of the reservoir as a result of increasing pore pressure. This will replicate injection of CO_2 into the reservoir. It is aimed to employ an exaggerated history with the parameters defined by project partners and other Work Packages within Sharp.

The duration of each stage is dictated by the drainage characteristics of the test samples. For reservoir sandstone the permeability is high and pore pressure oscillations can have a wavelength of less than 5 minutes. For low permeability clay-rich caprock, the wavelength could be more like one hour. Results from the PPO method are deemed best when at least 8 complete oscillations are used. This means that in reservoir rock each test stage can be one hour long, where as for caprock it needs to be 8 hours or more. The tests are expected to be run with intervals of 2 hours for reservoir material and 12 hours for caprocks. This means that reservoir rock test might be conducted in 15 days and caprock tests in 90 days. Therefore, reservoir rocks were tested first.

4.3   Test material

Careful consideration was given to what rock to test as part of the study. It was decided to use the same rocks that were used as part of the EPSRC Contain (The impact of hydrocarbon depletion on the treatment of caprocks within performance assessment for CO2 injection schemes; Harrington et al., 2018) project as they already have petrological and geomechanical data available, meaning that permeability and porosity could be mapped onto existing critical state mechanics models created for Staithes Sandstone, Bestwood Sandstone, and the Mercia Mudstone Group. However, this material was not derived from the North Sea and was selected as suitable analogue materials.

Potential core material from the Triassic Bunter Sandstone Formation (BSF) was identified at the National Geological Repository of the British Geological Survey. However, due to extensive slabbing and sub-sampling of these cores it was not possible to obtain samples of appropriate dimensions for experimental testing. As such, the Staithes Sandstone from the Chester Formation (part of the Sherwood Sandstone Group), was selected as the onshore analogue. It was decided that the material from the Staithes No.20 Borehole (NZ71NE/14;E476024, N0517997) would be appropriate. This core gave access to the Sherwood Sandstone Group between 650 - 925 m below ground level. This will be referred to as SSG1.

The Haighsborough is the offshore stratigraphic equivalent of the Mercia Mudstone Group (MMG). Samples from the MMG were collected from a depth of 57 m in the Carrickfergus salt mine, near Larne, Northern Ireland. The Larne Basin contains a Triassic sequence of various red beds of the Mercia Mudstone Group that have been

interbedded with evaporates, siltstones, and some sandstone beds (Downing et al., 1982). The experimental material belongs to the upper Knocksoghey Formation, a homogeneous, fine-grained, well-consolidated, reddish-brown mudstone, with abundant bluish-green patches of mudstone containing reduced iron. The lithological descriptions of the other formations in the basin do not significantly vary from the Knocksoghey Formation supporting the use of the material from Larne as an analogue for the Mercia Mudstone Group. However, the sample's petrographic description is less closely matched, suggesting that at a smaller scale the formation is more heterogeneous, which makes comparisons within the Larne basin and across the UK more complicated (Parkes et al., 2014).

In terms of the Northern North Sea material the Bestwood Sandstone, part of the Chester Formation of the Sherwood Sandstone Group, was selected as an analogue material for the Captain Sandstone. Nine samples of sandstone were prepared from blocks obtained from the Bestwood No. 2 Quarry located outside Papplewick, approximately 10 km north of Nottingham. The blocks were cut from approximately 30 m below ground level. This will be referred to as SSG2.

Another reason for the selection of the Staithes Sandstone (SSG1) and the Bestwood sandstone (SSG2) is their suitability as two end members of reservoir formations. Figure 4-4b shows a plot from Noy et al., in which porosity is shown against vertical air permeability for a number of sandstones. The Staithes Sandstone (SSG1) and the Bestwood Sandstone (SSG2) are plotted as lines at their measured porosities. As can be seen the Staithes Sandstone (SSG1) represents one end member as it has a relatively low porosity and therefore permeability. Whereas, the Bestwood Sandstone (SSG2) has a very high porosity and therefore plots as the opposite end member. Being able to measure hydro-mechanical data on two opposing end member reservoir rocks allows us to draw conclusions on the way in which a large range of reservoirs may behave during CO2 sequestration.
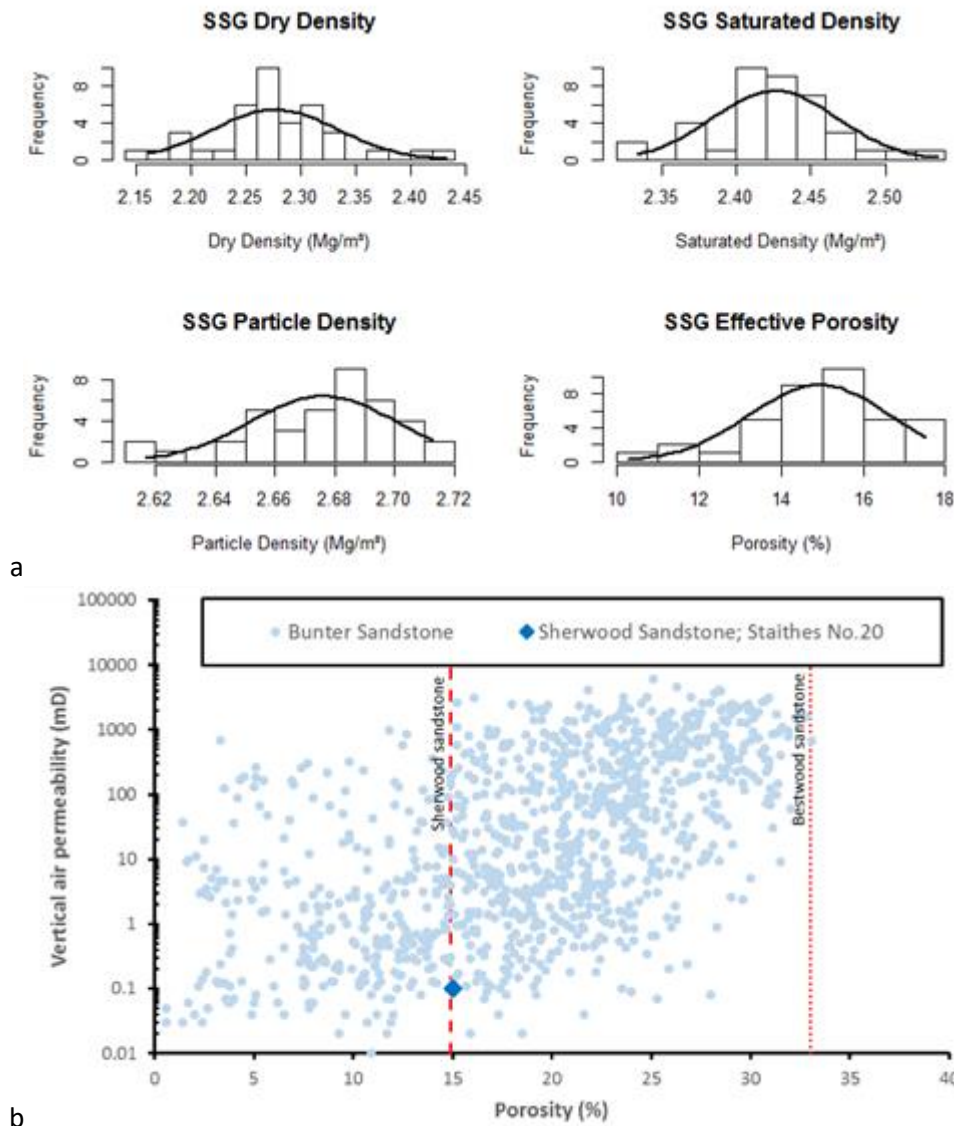
Figure 4-4 Sandstone physical property variability. a) Histogram and density plot for dry density, saturated density, particle density and effective porosity of the Sherwood Sandstone Group from the Staithes No. 20 borehole (SSG1); b) Vertical air permeability versus porosity for the Bunter Sandstone Formation (from Noy et al., 2012).

4.3.1   Sandstone deformation

Sherwood Sandstone Group 1 (SSG1): Figure 4-5 summarises the results from the compression tests for SSG1. A progression from brittle to ductile deformation was seen with increasing confining pressure. Examination of the final test samples suggested that the transition occurred at about 60 to 80 MPa confining pressure. All samples showed a peak in stress prior to strain-softening; generally, this peak stress increased with confining pressure, as described by a power law relationship (Figure 4-5b). However, the test conducted at 140 MPa confining stress, had a lower peak stress (303 MPa) than the test at 120 MPa (325 MPa). This may be due to differences in the effective porosity of the test samples, with the stronger test sample having a porosity of 14.8 %, compared with 16.5 %, or due to earlier onset of yield. Yield is the stress state when deformation transitions from purely elastic (recoverable) to plastic (permanent) behaviour. Some rock types show considerable difference between yield and peak strength. Reservoir properties start to change at the yield strength and therefore this stress state is of

significant interest. Post-peak stress behaviour also showed a clear transition from brittle to ductile behaviour. Samples tested at lower confining pressures (20 and 40 MPa) underwent Type II brittle failure; samples tested at intermediate confining pressures (60, 80, and 100 MPa) showed (sometimes considerable) post-peak strain-softening; samples tested at higher confining pressures (120 and 140 MPa) showed a transition to strain-hardening after an initial phase of post-peak strain softening. Strain results show that increasing confining pressure resulted in greater axial and volumetric strain at peak stress, with the exception of axial strain at 140 MPa, which is slightly lower than that at 120 MPa.
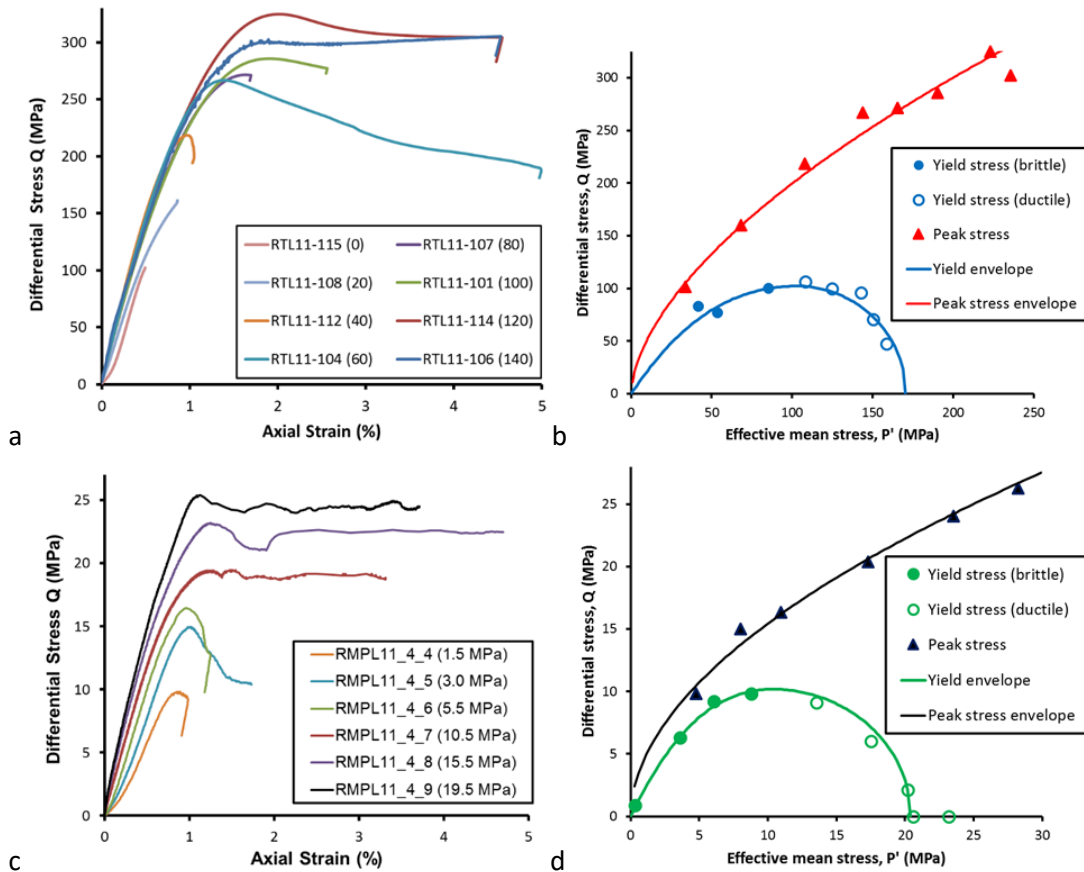

Figure 4-5 Results for triaxial compression testing of the Sherwood Sandstone Group (SSG1 and SSG2). a) stress-strain results for SSG1; b) yield and peak stress for SSG1 in P´ – Q space; c) stress-strain results for SSG2; b) yield and peak stress for SSG2 in P´ – Q space. Note: open yield stress markers denote deformation on the ductile side of critical state line and closed markers deformation on the brittle side.

Sherwood Sandstone Group 2 (SSG2): Figure 5cd summarises the results from the triaxial compression tests for SSG2. As with SSG1 a transition from brittle to ductile deformation was seen with increasing confining pressure, occurring at about 10 MPa confining pressure, much lower than seen in SSG1. Most samples showed a peak in stress prior to strain-softening, with the exception being test 7, which showed almost perfect elastoplastic behaviour. This suggests that 10.5 MPa corresponds with the brittle-ductile transition. Figure 4-5dshows that peak stress increased with increasing confining pressure, as described by a power-law relationship. On the ductile side of deformation, samples did not show any sign of strain-hardening even at elevated strains. This suggests that this sandstone variety can accommodate significant volumetric strains with relative ease. Inspection of stress-strain data at low confining pressures indicated Type II brittle

failure. Figure 4-5d also includes data from the two hydrostatic tests conducted, giving grain-crushing pressures (yield stress in a hydrostatic stress regime) of 20.6 and 23.2 MPa.

For both sandstones, Young's modulus increased with confining stress, although there is scatter within this relationship. Poisson's ratio was relatively constant throughout the pressure range with values between 0.16 and 0.2. For SSG1 at the lowest confining pressure a much higher Poisson's ratio of 0.35 was observed. This however, may be attributed to a high effective porosity of the sample (17.5 %), compared with the other test samples that ranged between 14.1 and 15.4 %. Mohr-Coulomb and Hoek-Brown (Hoek et al., 2002; Hoek & Diederichs, 2006) failure envelopes and corresponding failure criterion parameters were calculated for the triaxial and uniaxial compression tests, using the peak stress as peak strength and providing values for cohesion (c) and friction angle (Φ).

4.3.2 Yield envelopes

Yield was determined for each uniaxial, hydrostatic, and triaxial compression test. Yield was considered to be at the onset of significant stress deviation (more than 1 MPa for SSG1 and 0.1 MPa for SSG2) from the tangent of the elastic region of the stress-strain curve. Error in determining yield was not significant and generally varied by less than 10 % when different sections of the stress-strain curve were considered linear.

Figure 4-5d,b shows the results for yield and peak strength when plotted in the differential (Q) versus effective mean stress (P') space. Differential stress was calculated as the difference between axial (σ_1) and confining stress (σ_3). Effective mean stress was defined as $^1/_3(\sigma_1 + 2\,\sigma_3) - Pp$, where Pp is pore-pressure. As seen, the peak strength data for both SSG1 and SSG2 follow a curved trend with strength continually increasing with mean stress as a power-law. Yield showed a curved form. For tests that displayed shear-localisation in hand specimen (dilatant behaviour), the data fall on the portion of the curve with a positive slope. For tests with pervasive cataclastic flow (contraction), the data fall on the portion of the curve with a negative slope. The apex of the yield envelope signifies the condition of isovolumetric deformation, also referred to as critical state deformation or the brittle-ductile transition.

The post-test observations of failure mode showed that the transition from brittle to ductile deformation occurred between 60 and 80 MPa for SSG1 and around 10.5 MPa for SSG2. On the brittle side, purely brittle deformation was seen with sample failure by shear localisation. Around the brittle-ductile transition a more distributed series of localised deformation features formed. At elevated confining pressures the samples appeared to have undergone distributed ductile deformation with the test sample clearly barrelling. These observations are consistent with those of Wong et al. (1997) and Cuss et al. (2003). For SSG1 it should be noted that the brittle-ductile transition at such a pressures represents a depth greater than 2.5 km in the Southern North Sea, which is deeper than the depth of most potential storage sites in the area. Therefore, SSG1 is not likely to undergo distributed cataclastic flow (contraction) and that deformation would be brittle (dilatant), or at the brittle-ductile transition (isovolumetric). However, for SSG2 the brittle-ductile transition represents a depth of less than one kilometre and therefore deformation would be possible by either dilation or contraction under a variety of stress conditions.

Limited yield data is available in the literature, particularly for weak sandstone varieties. However, data from 27 individual studies covering Adamswiller, Berea, Benteim,

Bestwood, Bleurswiller, Boise, Darley Dale, Diemelstadt, Hollington, Kayenta, Penrith, Rothsbach, Sherwood, and Tennessee sandstone varieties was found in papers by Baud et al. (2004, 2006), Cuss et al. (2003) Fortin et al. (2006), Klein et al. (2001), Louis et al. (2009), Rutter & Glover (2012), Wong & Baud (2012), Wong et al. (1997) and Zhu et al. (1997).
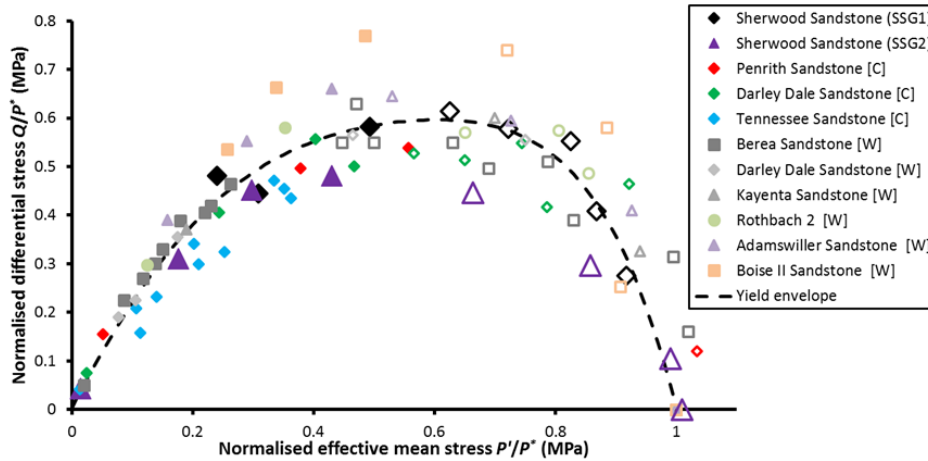

Figure 4-6 Critical state envelope calculated for 11 sandstone varieties, normalised by the grain crushing pressure (P*). As seen, all data approximately correspond to a single yield envelope with brittle deformation below P´/P* = 0.5 and ductile deformation above. [C] refers to Cuss et al. (2003); [W] refers to Wong et al. (1997); open symbols denote ductile deformation; closed symbols denote brittle deformation.
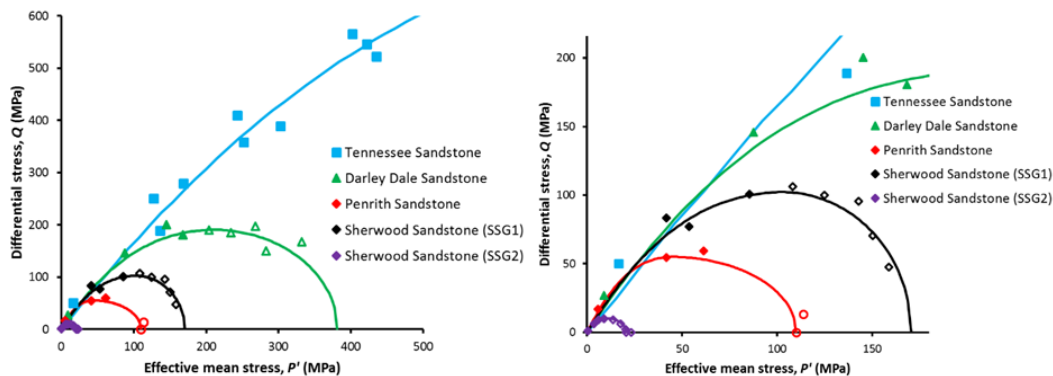

Figure 4-7 Comparison of the current test data (Sherwood Sandstone Group SSG1, SSG2) with Penrith, Darley Dale and Tennessee sandstone (from Cuss et al., 2003). Open symbols denote ductile deformation; closed symbols denote brittle deformation, solid lines represent the calculated yield envelopes.

Figure 4-6 shows data from the current study compared with the results presented by Cuss et al. (2003) and references therein. Wong et al. (1997) showed that sandstones when normalised by their grain crushing pressure (P*) have a similar, singular, yield envelope. The grain crushing pressure is the condition where yield occurs under purely hydrostatic conditions and in a Q-P plot occurs along the abscissa. This was achieved in SSG2, but was greater than that rating of the apparatus for SSG1. However, the grain crushing pressure can be determined from the Hertzian contact model (Wong et al., 1997), which states P* scales with the grain radius (R) and porosity (ϕ), such that:

$$P* \quad [1]$$

Average grain diameter and porosity were determined to be 215 µm and 15 % respectively using scanning electron microscopy. This gave a predicted P* of 173 MPa, allowing the current study to be normalised and plotted in Figure 4-6. The current data correspond well with the findings of Wong et al. (1997) and Cuss et al. (2003). This is further emphasised in Figure 4-7 where the current data for SSG1 and SSG2 are compared with Penrith, Darley Dale, and Tennessee Sandstone varieties (from Cuss et al., 2003). SSG1 is intermediate in strength between Penrith and Darley Dale Sandstone, whilst SSG2 is the weakest of the five rock types.

4.4   SHARP experimental results to date

The test programme consists of a minimum of 6 tests, with an option for four more depending on progress Table 4-1. Tests will be conducted on Bestwood Sandstone (reservoir), Staithes Sandstone (reservoir), and Mercia Mudstone (caprock). If time allows two varieties of loose sand will be tested, although this will require modification of the apparatus, which requires availability of the BGS Engineering Workshops.

The SHARP project started with several calibration experiments to determine the optimum experimental parameters (length of test stages, wavelength of oscillation). This included tests using Staithes Sandstone and Boom Clay, a similar plastic clay to Mercia Mudstone. Boom Clay was selected as plenty of well-preserved core was available.

Following the calibration tests, the first test was conducted using Staithes Sandstone. This test was conducted between 15/12/22 and 4/1/23. Unfortunately, this test suffered leakage from both confining and pore pressure pumps. The former resulted in the syringe pump not being able to continue to change confining pressure and the system slowly drained. The leakage of the pore pressure system meant that reliable porosity data was not easily calculated. As a result, the test was repeated. The first test will be processed based on the learnings of the second and is awaiting processing at BGS by a modelling member of staff.

Table 4-1 Planned experiments

	Rock type	Geological history	Engineering history
1	Bestwood Sandstone	Sh_01	Sh_04
2	Staithes Sandstone	Sh_02	Sh_05
3	Mercia Mudstone	Sh_03	Sh_06
(4)	Loose sand 1	Sh_07	Sh_09
(5)	Loose sand 2	Sh_08	Sh_10

4.4.1   Test Sh_02 – Staithes Sandstone

The second test was a successful test conducted on Staithes Standstone. The test sample was 49.93 mm in diameter and 25.72 mm in height, with a weight of 132.05g. The test started on 26/1/23 and was completed on 24/2/23.

Figure 48a shows the porosity of the sample as determined from the syringe pump volume. It must be noted that the starting porosity is that determined for the sample at

atmospheric pressure and not that seen at 2 MPa effective stress. What can clearly be seen is that the sample shows considerable influence of stress history. As confining pressure was increa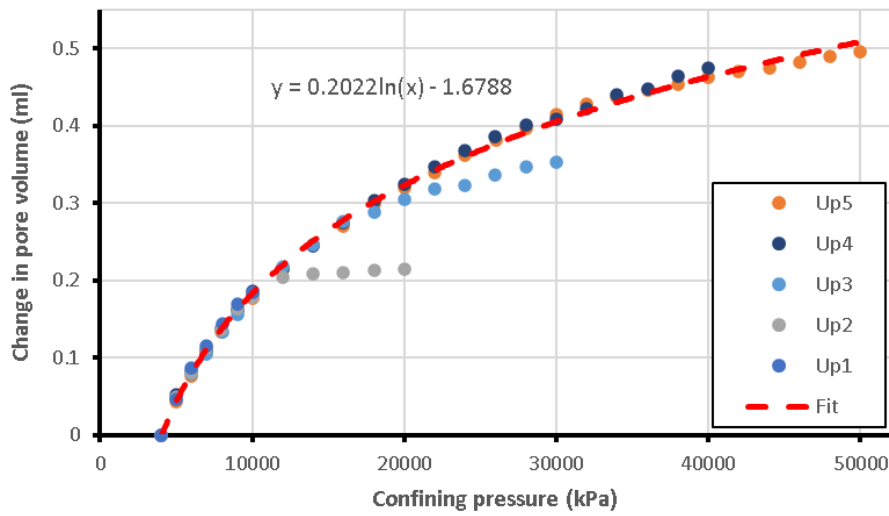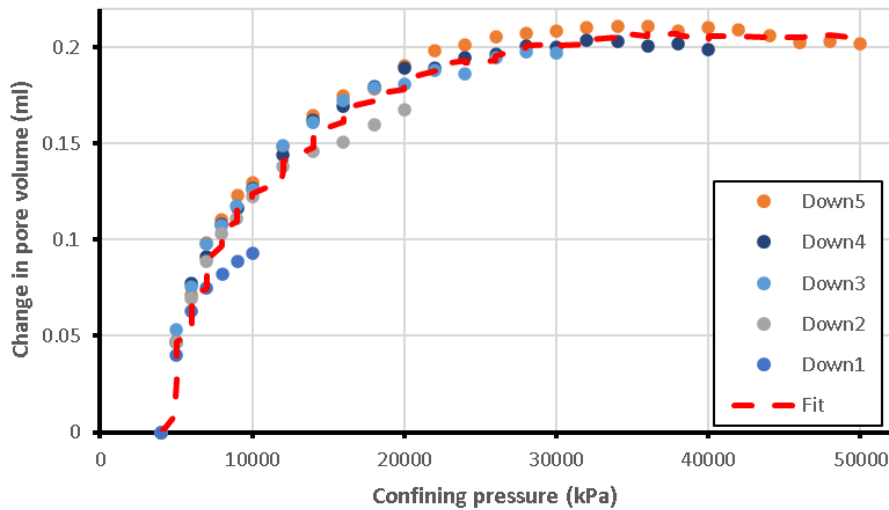sed, porosity reduced. As confining pressure was reduced, porosity increased, but not at the same rate as the loss of porosity from pressure increase. This is observed at all cycles followed. Figure 4-8b shows the change in pore volume just for the increasing pressure steps. As can be seen, the five cycles generally show the same trend that can be described by a logarithmic fit. However, in detail Up2 and Up3 showed slightly different trends when the maximum pressure of the previous cycle was reached. The reason for this is not known. The down cycles (Figure 4-8c) also show a similar trend to one another, but one that does not match the up cycles. These data are not described by a logarithmic trend and for display purposes have been shown with a moving average. The difference between the two relationships is the result of stress history. It can be seen that during up cycles a total of 0.5 ml is lost by 50 MPa, whereas only 0.2 ml is recovered during the down cycle. It can also be seen that the trend for the up cycle suggests that higher confining pressure will result in further porosity loss, whereas the porosity recovered during the down cycle had reached plateau by 30 MPa. This suggests that higher pressure cycles would not result in any more porosity recovery and the influence of stress history will become more marked. The origin of the hysteresis is not known and is the focus of further investigation during the remainder of the project.
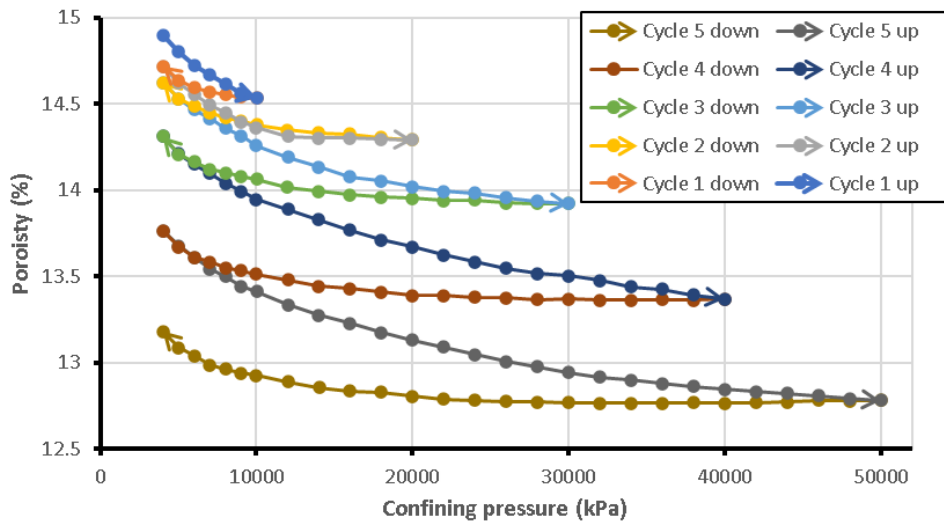
Figure 4-8 Porosity of Test Sh02 (Staithes Sandstone). a) Porosity; b) Change in porosity during increasing confining pressure; c) Change in porosity during reducing confining pressure.

Figure 4-9 shows the preliminary permeability result for the test. This shows that permeability showed variation during the confining pressure cycles. However, the data is quite noisy and shows permeability increasing, while confining pressure was increasing. Further investigation is needed to confirm this observation as permeability is expected to decrease while porosity decreases. The data show stress history, as seen

by a decreasing minimum permeability. However, it can be seen that the change seen in the fifth cycle is less than that seen in the fourth cycle. It is expected that the data can be better refined and as such this result is considered preliminary until further investigation occurs.
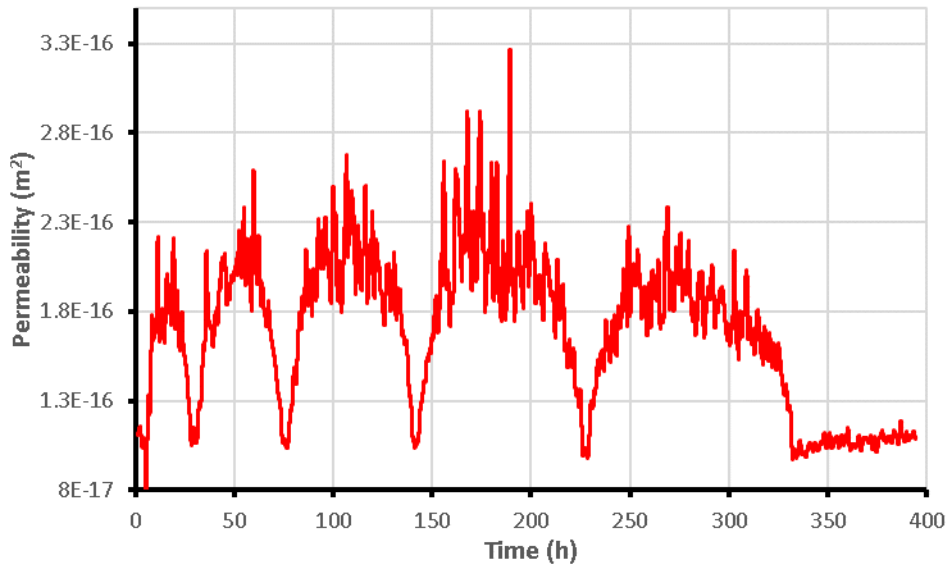
Figure 4-9 **Permeability of Test Sh02 (Staithes Sandstone).**

4.4.2   Test Sh_01 – Bestwood Sandstone

A sample of Bestwood Sandstone has started testing. However, the weak nature of this sandstone meant that a perfect cylinder sample was not achieved, and this resulted in jacket failure during testing. A solution has been engineered and a new test sample will be manufactured, and the test re-started. The high porosity and weak nature of this sandstone means that permeability is high and close to the limit of the apparatus. However, Bestwood Sandstone is expected to yield at an effective stress of around 20 MPa and should result in considerable permanent change in porosity and permeability.

4.5   Outlook

It is planned to conduct the four tests on reservoir rock (Staithes and Bestwood Sandstone) before moving to the caprock material, which will take significantly longer time to conduct. If time permits, loose sand will be tested. The permeability data, as determined from the PPO method will be further refined to achieve less noisy results. The relationships seen in porosity and permeability change will be mathematically defined to create an equation where porosity can be predicted knowing a stress history.

5 Discussion

5.1 Methodology for stress estimation based on lithology

5.1.1 Empirical framework

Various empirical relations relating K_0 to volume of clay content (V_{cl}), Plasticity index (I_p) and water content (w_i) have been established and tested. The choice of method depends on which type of data is available and knowledge of the mineralogy (i.e. whether plastic clays like smectite is likely to be present or not). In Quaternary sediments where Ip is typically characterized, I_p may be used directly. However, for Norwegian quaternary clays with limited range of plasticity, the relation using OCR only may be applicable (L.Heureux, 2017). There were very limited mineralogy data from the geotechnical site investigations, and hence correlation for specific minerals like smectite is still in lack of good datasets. This can be improved if addressed in systematic studies in future work.

Equations established under SHARP and recommended for further use are listed in Table 5-1. The Equation number refers to those listed in Table 2-2. Eq. 2, 4 and 15 are suggested to define K_0 in normally consolidated area (K_0_nc) which is believed to be fundamentally linked to the initial friction angle during initial deposition and mechanical compaction of sediment. Eq.4 requires I_p which can be obtained indirectly from content of clay and smectite from Eq. 16 or 17, respectively. Once K_0_nc has been derived, potential effect from uplift can be derived from Eq. 18 or 19 based on low or high plasticity clays, respectively. These equations are limited to the mechanical compaction regime (<2km maximum burial depth, ideally even shallower with < 1km burial depth) corresponding to a transition from mudstone to shale where diagenetic effects and cementations start to develop.

Table 5-1 Relationships for estimating K_0 for clays, mudstone and shales. Equation number refers to equations in *Table 2-2* and Chapter 3.

K_0	Eq.	Equation	Comment
K_0_nc normally consolidated (Eq.16)	2	$K_{0\_nc}=0.95-sin\varphi'$	effective friction angle of remoulded material
	4	$K_{0\_nc} = 0.33(Ip)^{0.17}$	From I_p directly when available, alternatively from Eq. 18.
	15	$K_{0\_nc}=((0.034 \cdot V_{cl}+0.3681) + (0.003 \cdot V_{\_smectite}))$	Shown in Figure 2-4. Reference Grande et al., 2022.
	18	$I_p = 0.7995 \cdot V_{cl}$	For use in Eq.4.
K_0_oc Over consolidated (Eq.17)	24	$K_{0\_oc} = K_{0\_nc} \cdot OCR^{0.47}$	For low plasticity clays and mudstones <1km max burial depth
	25	$K_{0\_oc} = K_{0\_nc} \cdot OCR^{0.39}$	For high plasticity clays and mudstone <1km max burial depth

The methodology is demonstrated for clays and shales in the Horda Platform area and are further discussed for the Lisa field based on information on mineralogies of relevant lithologies.

5.1.2 Lithological bounds for K_0

The observed range of K_0 from laboratory data on synthetic and natural clay, silts, and sands during mechanical compaction (normally consolidated state, uniaxial compaction) as presented in the Figure 2-3 and Figure 2-4 generally falls within range 0.4-0.8. Interpreted K_0 from majority of XLOT data in Norwegian Continantal Shef falls within the same range of 0.4-0.8 (Andrews et al., 2016 and Thompson et al., 2022). Cumulative

probability plots of derived Ko value from XLOT tests, based on observations from 148 high quality XLOT test in Norwegian Continental with bounds for expected lithological impact from mechanical compaction is shown in Figure 5-1. The lithological bounds of K_0 are indicated with a low bound of 0.4 corresponding to 100% sand and high bound of 0.8 corresponding to 100% clay. The data are plotted for all depths (a) and depths 1< km (b). The cumulative distribution is slightly wider when including all depths (a) compared to depths < 1km (b).
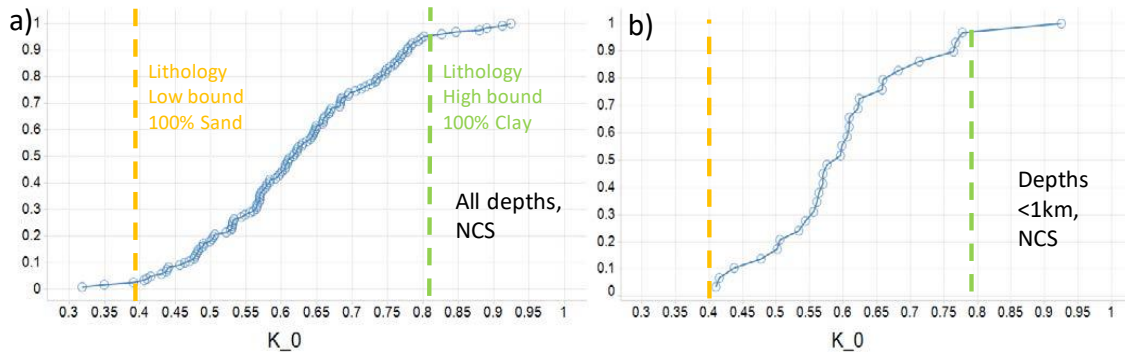

Figure 5-1 Cumulative probability plots of derived Ko value from XLOT tests, based on observations from 148 high quality XLOT test in Norwegian Continental Shelf (NCS)- (background figures from Andrews et al., 2016). The lithological bounds of K_0 for normally consolidated state are indicated with a low bound of 0.4 (corresponding to 100% sand) and high bound of 0.8 (corresponding to 100% clay). The data are plotted for all depths (a) and depths 1 < km (b).

Most XLOT data are from siliciclastic rock with a majority in impermeable clay rich mudstone and shale intervals and consentrates around K_0 of 0.6. There are also few data with K_0 down to 0.3 and up to 0.95. It should be noted that observed variation range from XLOT may not be from impact of lithology alone, as uplift, excess pore pressure and tectonics can impact on the distribution. However, litholical bounds for normally consolidated state of K_0 is a useful indicator for what K_0 we may expect from impact lithology variations in a subsiding relaxed basin. The concept of lithological bounds has ben demonstrated in summary plots of field stress data for fieldcases in Report DV1.2.

5.1.3   Plaseticity (Ip) and Smectite rich units in the North Sea

Among the typical clay minerals, plastic minerals like smectite are found to have high impact for the K_0 ratio. In this chapter we therefore include some more detail of how smectite rich layers are distributed in North Sea lithologies, giving context to fields and areas where they should be considered in stress characterisation workflows.

Smectite content is most often not known from log methods and needs to be characterized from XRD or QEMScan of core or cuttings material. However, knowledge from regional geology may be useful if chronostratigraphic information of the formation(s) is available. This section includes some regional understanding of the abundance of Smectite in the North Sea tertiary sediments.

Smectitic mudstones, mostly of Lower Tertiary age, and in particular Eocene and Oligocene mudstones representing distal facies, may have a very high smectite content (>50%) and almost no quartz or feldspar (Hugget, 1992, Bjørlykke, 1998, Bjørslev Nielsen et al., 2015). These mudstones are derived from volcanic ash resulting from subaerial volcanicity during the opening of the Norwegian-Greenland Sea. Mudstones of more proximal facies contain more kaolinite and quartz (Bjørlykke 1998, Rundberg, 1989). Eocene and Oligocene mudstones with high smectite content are characterized

by low V_p (<2 km/s) and bulk densities compared to mudstones with other mineral assemblages at the same burial depths, and velocity inversion is often observed (i.e., compared to Pleiocene and Pleistocene mudstones where V_p are often in the range 2.5-3 km/s (Marcussen et al., 2010. Such smectite-rich mudstone, in combination with high uplift, may give significantly higher K_0 from impact of the high plasticity or indirectly from high pore pressure due to low permeability in these formations.

Clay mineral compositions have been analyzed in samples from the Danish, Norwegian, British, and Dutch North Sea sectors and from onshore Denmark and Germany, comprising both wells and outcrops (clay pits and cliff sections) (Bjørslev Nielsen et al., 2015). The time slices investigated comprise the Paleogene, the post-Ekofisk Fm. interval of the Paleocene, the entire Eocene, and the entire Oligocene. The distribution of the most dominant clay minerals—smectite, chlorite, kaolinite and illite—are shown on maps comprising the Paleocene, Eocene, Oligocene, and the formations Vejle Fjord Fm., Klintinghoved Fm., Arnum Fm., and Gram Fm. from the Miocene. Example of a map from Oligocene is shown in Figure 5-2, and the Horda Platform east-west cross section and Lise field are indicated in the map. For Horda platform, wells from Troll in East (31/6-1) to Martin Linge in west (29/9-1) have been included in the analysis which is the basis for the contour maps. A further discussion and relevance of these high plasticity units are described for Horda Platform and Lisa respectively.
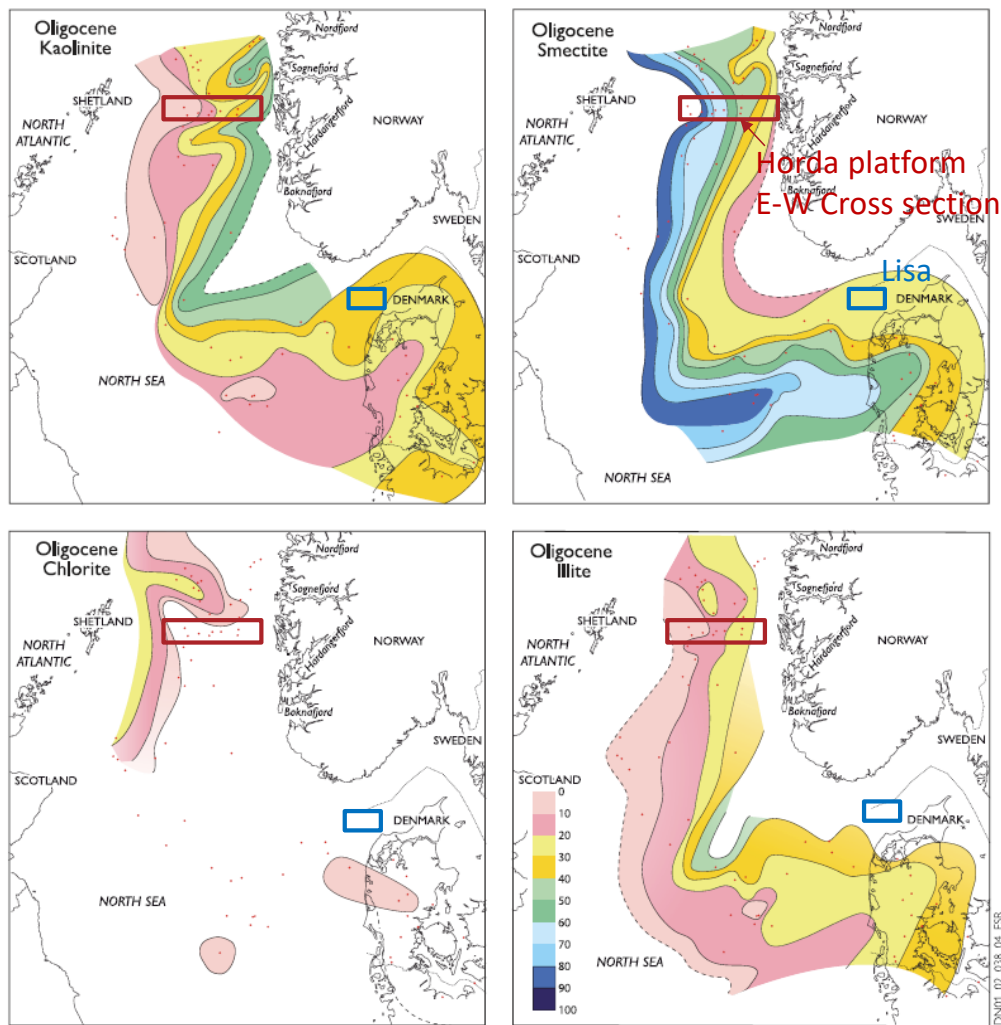

Figure 5-2 Distribution of clay minerals in the Oligocene succession. Note: higher amounts of chlorite to the north supplied from the Shetland area and its sporadic presence to the south. Kaolinite supplied from Norway. Substantial illite supplied from SW Norway. Smectite dominance in central parts of the basin. Values are in % (Bjørslev Nielsen et al., 2015).

5.1.4 OCR- Over consolidation ratio in North Sea sediments

Overconsolidiation ratio can vary based on erosion and uplift, glacial loading, tectonic events throughout during geological history and details on this subject has been discussed in SHARP DV1.1b and DV1.2 reports. It also depends not only on the load experienced load but also the loading ratio and the ability to drain the sediments, and whether excess pressure were developed throughout the load history preventing compaction. Chemical compaction and diagenetic effects can lead to pseudo-overconsolidation. Values of OCR are typically largest in shallow units i.e. quartenary units and OCR up to 8 is quite common from Ice loading.

5.1.5 Comments and limitations in methodology

This study focuses on siliciclastic sediments ranging from clay and sand to mudstones and shales dominated by clay minerals illite, kaolinite, smectite and quartz. The quaternary sediments are rich in silt with low smectite content and rather low plasticity. The example shales Lista, Shetland and Draupne have a maximum 10-15% content of smectite. The Eocene smectite rich sediments can have large smectite content up to 80% of clay fraction (i.e. Bjerslev Nielsen, 2015). Halite, chalks and other carbonate rich sediments and rocks are not analysed herein, although they are relevant elsewhere in the North Sea basins and particularly at Endurance and Aramis fields. Other relations may be valid for such formation. This is especially the case for Halite which creeps when subjected to elevated stress and temperature (giving a $K_0 = 1$).

A main limitations in this method is the assumption of uniaxial strain which may not be valid if the basin is subjected to more complex stress history. However, although extensional stresses have been active throughout early sedimentation history in North Sea (see SHARP Report DV1.1b), interpreted K_0 from majority of XLOT data in Norwegian Continantal Shef falls within the range of 0.4-0.8 (Andrews et al., 2016 and Thompson et al., 2022) also shown in Figure 5-1. The observed variations of K_0 in the Horda platform, which is hydrostatically pressured and dominated by siliciclastic sediments, may therefore to a large extent be explained by variations in the natural variations in composition of sediments including uplift and glacial erosion. The K_0 from XLOT data may however be larger or smaller if overpressured systems typically below 3 km (see Report DV1.2 report and Thompson et al., 2022b). A more complex stress history is expected in Endurance and in the Aramis fields (see WP1, D1.1a and b reports).

Another limitation related to uniaxial strain conditions is that the sedimentary layer should have a significant lateral extent for these stresses to develop following uniaxial strain boundary condition. This may not always be the case in different sedimentary facies or across structural boundaries. If the sediment has limited lateral extent or thickness, then averaging of stress based on the main lithologies presents over a certain vertical interval may be needed to account for local strains. An understanding of the lateral distribution of layers from seismic will be beneficial, and the method of lithological impact should be used together with geological knowledge of the involved formations.

6 Testing method on Field cases

6.1 General

In this chapter, we have estimated K_0 based on empirical relationships using information on effective friction angle of remoluded material, mineralogical information, content of clay, smectite and overconsolidation ratio (OCR). The methods are demonstrated on the Hordaplatform where estimated K_0 from mineralogy of reference lithologies from lab tests (Quarternary, Hordaland, Lista, Shetland, Draupne and Drake) are compared with K_0 from field stress XLOT data (Hordaland, Draupne and Drake). Furthermore, an evaluation of lithological impact on stress is also tested on the less mature Lisa field (DK) where field specific LOT or XLOT data are not yet available, and prediction is based on regional mineralogy, LOT data and reginal uplift. Regional trendlines from North Sea and bounds for expected lithological impact are tested on LOT tests from Denmark (see Report DV1.2). A further demonstration of laboratory based data and relations applied on logs and constitutive models and calibration with field stress XLOT and LOP data is shown in Report DV1.2 and Grande et al (2022).

6.2 Horda platform field case (NO)

Examples of the application of the methodology for the reference clays and mudstones are shown in Table 6-1. Further information on mineralogy for mudstone samples is shown in Table 2-1, and more alternative Equations are shown in Table 2-2.

Table 6-1 Estimated K_0 based for reference clay, mudstone and shales based on information on content of clay content (V_{cl}), smectite (V_{sme}), friction angle of remoulded material (φ) . Porosity (ϕ) and Unit weight (Y) are reported as a reference. The Equations for K0 applied in this table is listed in Table 5-1.

Fm.	Depth m TVD bsf for CD and (MBD)	Further Input for K_0 equations					K_{0_nc} Normally consolidated			K_{0_ocr} Over-consolidated	
		V_{cl} %	V_{sme} %	Ip (Eq. 17 [1]) %	OCR	φ (^{o})	Eq. 2	Eq.4	Eq. 15	Eq. 4 and 19	Eq. 15 and 18
Q Unit I	0	44	5.72	37	1.45	-	-	0.61	0.53	0.70	0.64
Q Unit II	16.5	26	3.38	20	1.55	-	-	0.55	0.47	0.65	0.57
Q Unit IIIa	74	7	0.7	15	7	-	-	0.52	0.39	1.12	0.98
Q Unit IIIb	110	26	2.6	28	2.35	-	-	0.58	0.46	0.81	0.69
Q Unit IV	135	69	8.97	38	2.55	-	-	0.61	0.63	0.88	0.98
Unit V Oligocene	201	36	21.6	50	2.55	-	-	0.64	0.56	0.92	0.86
Lista	782 (1182)	25	12.5	(18.7)	1.39	-	-	0.54	0.49	0.64	0.60
Shetland	906 (1306)	45	7.5	(39.4)	1.35	-	-	0.63	0.57	0.72	0.68
Draupne	1000 (1400)	50	5	(36.8)	1.32	18.8[2] (22.3)	0.63[2] (0.57)	0.62	0.55	0.71	0.65
Drake	2245 (2545)	61 (85)	9	13	1.12	25.8	0.51	0.51	0.60	0.53	0.64

[2] Values of Ip in parenthesis are calculated with Eq. 17, for others Ip is measured or reported directly.

[2] Based on friction angle at onset and residual failure of remoulded material, residual in parenthesis.

A summary of the XLOT/LOT derived K_0 values in the main sealing formations, Drake and Draupne, for wells in the eastern part of the Horda platform is presented in Grande et al. 2022. The K_0 based on the depth of XLOT values as predicted from gammaray log method are shown in SHARP DV1.2 report. Predicted K_0 from mineralogy data from core tests compared with measured K_0 from XLOT field test is shown in Table 6-2 Predicted K0 from mineralogy data from core tests compared with measured K0 from XLOT field test. The reference OCR value at depth of XLOT is also shown for completeness. This value is estimated based on pre-consolidation stress calculated from uplift estimates from exhumation study (DV1.2) using an average density of 2.0 g/cc of eroded rock and assuming hydrostatic pressure (see Grande et. al 2022 and SHARP report DV1.2).

Table 6-2 Predicted K0 from mineralogy data from core tests compared with measured K0 from XLOT field test (XLOT data from Report DV1.2). Note: Mineralogy is not from the same depth and well as XLOT (except Drake)

Fm.	Depth info m MD (m MBD)	K0 from XLOT	K_{0_nc} Normally consolidated predicted					
			OCR at depth of XLOT	Eq. 2	Eq.4	Eq.15	Average Eq. 2, 4 and 15	Difference $(K0_{Pred\_Avg} - K_{0\_XLOT})/ K0_{XLOT}$ %
Unit V Oligocene (Troll West)	607 (807)	0.56	1.34	-	0.64	**0.56**	0.6	7.1
Shetland (Oseberg)	2631 (2631)	0.61[1]	1.0	-	**0.63**	0.57	0.6	1.6
Draupne (Eos and Smeaheia Gamma)	1559 (1859)	0.63	1.18	**0.63*** (0.57)	0.62	0.55	0.6	-4.8
	852 (1852)	0.54	2.19	0.63* (0.57)	0.62	0.55	0.6	11.1
Drake (Eos)	2283 (2583)	0.4 (0.55)[2]	1.12	0.51	0.51	0.60	0.54	35.0 (-1.8)

[1] XLOT from Oseberg, and mineralogy from Troll East well
[2] Alternative interpretation of K_0 from XLOT test (Thompson et al 2022a).

The difference between average predicted and measured K_0 from XLOT is +/-11%, except for uplifted Drake Fm. low value (K_0 =0.4) where difference is 35%. The differences varies slightly between methods and so an average of the estimation methods is used. The OCR term was not applied to any of these cases and would result in an overestimation of K_0. A detailed discussion of all lithologies, including XLOT, LOP and log analysis data are given in Report DV1.2. A discussion of Drake and Draupne Fm.s is also given below with a reference to numbers presented in Table 6-1 and Table 6-2, here with focus for the impact of lithology and the normally consolidated behaviour during process of mechanical compaction. This discussion is overlapping slightly with report DV1.2.

Drake Fm (Eos):
XLOT in the Drake formation indicate a K_0 of 0.4 with an alternative interpretation of 0.55 (Thompson et al., 2022a). The calculated value of K_0 was 0.51 from measured friction angle of 25.8° and plasticity Ip of 13% of remoulded/reconstituted Drake shale material (Eq. 2 and Eq. 4). Calculated K_0 was 0.6 based on V_{cl} of 61% and from XRD data

from same core and using $V_{smectite}$ of 10% ($V_{Smectite}$ of 6-9% is reported from QEMSCAN)(Grande et al., 2022). For Draupne shale Calculated average value of K_0 for NC state is 0.54, only 1.8% less than high value reported from XLOT 0.55. In comparison, the friction angle and cohesion of intact Drake from undrained triaxial shear tests is 24.8° and 5.95MPa respectively (Griffith et al 2022, CO2 DataShare), and friction angle is close to the remoulded effective friction angle in this case. When comparing to reference clays from literature, the measured I_p and $V_{smectite}$ of Drake falls somewhere in between Chicago clay (V_{cl} =65%, $V_{smectite}$ =6%, Ip of 10.3% and K_0 of 0.48) and Weald Clay (V_{cl} =70%, $V_{smectite}$ 10.6%, Ip=20% and K_0 = 0.54) (Brooker and Ireland, 1965, see Table 2-1). From empirical correlations and reference clays, we may therefore argue that a K_0 in range 0.48 to 0.60 is reasonable for normally consolidated state of Drake based on mechanical compaction, and the high-end value of 0.55 from XLOT test is then reasonable value. A further correction of K_0, based on the uplift of 0.3km and the corresponding OCR of 1.12 at the depth of XLOT, is likely not relevant for deep sandstones that experienced diagenesis (see SHARP Report DV1.2, DV1.3 and Grande et al. 2022).

The low value of K_0 of 0.4 are more in-line with normally consolidated state of sand, and some alternative mechanisms for such low value may be 1) diagenesis combined with uplift, 2) K_0 influenced by underlying sand rich Cook and Johansen Fm's sandstones or 3) tectonic extensional component from uplift. These mechanisms are further discussed in DV1.2 and DV1.3

Draupne Fm (Eos and Smeaheia gamma):
For Draupne Fm., K_0 of 0.63 and 0.54 are reported based on XLOT tests in Eos well (Thompson et al 2022a) and Smeaheia gamma well (Wu et al., 2022) respectively. The calculated K_0 are in range 0.57-0.63 based on friction angles in range 18.8-22.3° as measured on reconstituted Draupne shale from Ling depression (from Eq. 2 in Table 6-1). K_0 of 0.62 and 0.55 were calculated from Ip (Eq.4) and V_{cl} and $V_{smectite}$ (Eq. 15), based on mineralogy data from Smeaheia Alpha and Beta well (Rahman et al., 2020) and Ling Depression (Skurtveit et al., 2014). V_{cl} and TOC are reported to V_{cl}= 66 and 70% and TOC= 2.78 and 2.81 for Alpha and Beta well, respectively (Rahman et al., 2020). Draupne may then be comparable with Weald Clay (V_{cl}=70%, $V_{smectite}$ 10.6%, Ip of 20% and K_0= 0.54 (Brooker and Ireland, 1965, see Table 2-1), close to measured K_0 from XLOT test in Smeaheia gamma. From empirical correlations and reference clays, we may therefore argue that K_0 values in the range 0.54 to 0.63 are reasonable for normally consolidated state of Draupne shale during process of mechanical compaction, and values both values of K_0 of 0.54 and 0.63 reported from XLOT tests falls within this range.

In Eos well, Draupne experienced limited uplift (0.3km, OCR=1.18), while in Smeaheia Gamma well east of Eos, Draupne are more uplifted (1km, OCR=2.19), however, their maximum burial depth may be similar and in order 1.9 km. If assuming similar mineralogical composition of Draupne in the two sites, the K_0 after mechanical compaction may correspond to a high value of 0.63 at their maximum burial depth of 1.9 km (using K_0 from Eos, close to normally consolidated) and a then a net reduction from 0.63 to 0.54 from the 1km uplift in Smeaheia Gamma. Such a scenario would indicate that diagenesis and chemical alteration of rock may have lowered the K_0 at the during the process of uplift. Further testing of diagenetic behavior is shown in SHARP report DV1.2 and DV1.3.

6.3 Lisa field case (DK)

There is not yet any field stress data from the Lisa field specifically. However, LOT data from Denmark has been collected and plotted with depth in the SHARP DV4.1 report. In this report and SHARP Report DV1.2, we discuss the application of the empirical knowledge from WP1 and WP2 work so far and compare with trendlines for North Sea (Thompson et al., 2022b). Thus, Lisa is a good example of applying regional knowledge from more mature to less mature areas.

Geological setting and stratigraphy

The main sandstone reservoir for CO_2 storage in the Lisa structure is the Upper Triassic–Lower Jurassic Gassum Formation, with the Lower Jurassic Fjerritslev Formation forming the seal. The structure is penetrated by the J-1 well which was drilled in 1969 and reveals a thickness of the Gassum and Fjerritslev formations of 199 and 623 m, respectively (Figure 6-1). The well intersected the top of the Gassum Fm in 1697 m below msl., a few tens of meters below the apex of the Gassum Fm closure.

The Gassum Formation is widespread in the Norwegian–Danish Basin (Figure 6-2) where it in general has a thickness of 30–150 meters (Nielsen & Japsen 1991, Nielsen 2003). Locally it is missing due to uplift and erosion related to regional uplift in the Middle Jurassic, at the ˈBase Middle Jurassic unconformityˈ or the ˈMid-Cimmerian Unconformityˈ *sensu* Nielsen (2003), and within

The mineralogical maturity of the Gassum Formation varies across the Danish area. The formation can thus be divided into a region in East Denmark of high maturity with high quartz content and a region in NW Denmark with a less mature composition with higher e.g., feldspars (Figure 6-3) (Olivarius et al. 2022). The Gassum Formation in the Lisa structure belongs to the northwestern region with the less mature composition. Unfortunately, no cores are available from the formation in the J-1 well or nearby offshore wells. Consequently, core material from onshore wells in the northwestern area are used as analogues (Figure 6-5). The exception is a core from the Stenlille-6 well in central Zealand (the region of high maturity) which is included for comparison.
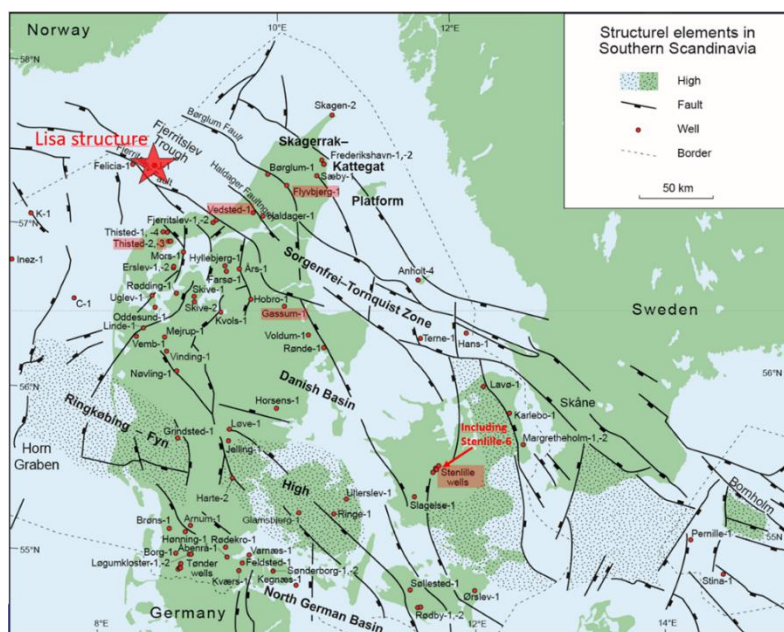

Figure 6-1 Map of wells

The Fjerritslev Formation, forming the seal, is a succession of marine claystones and mudstones, interbedded with thin sandstone units. The bulk mineralogy of mudstones (X-ray diffraction analysis) from the Fjerritslev Formation shows quartz as the dominant mineral followed by kaolinite and illite or mica. Feldspars are present in some samples. Also, calcite, siderite or pyrite are present in some samples, mainly in the mudstones. Clay mineral analyses from the formation are few. Ten samples from the Fjerritslev Formation in Kvols-1 (central Jutland) show little variation through the formation (Figure 6-5). All samples are dominated by kaolinite, followed by mixed-layer minerals, vermiculite and mica (Vosgerau et al. 2016). TOC-values from Kvovls-1 are generally very uniform, c. 1 wt. %.

The Lisa Structure is located at the edge of a basement high bounded by a large basement fault in the Sorgenfrei-Tornquist zone. Very little borehole breakout work has been done on Danish wells (Figure 6-6).

Table 6-3 Depths and thickness of Gassum and Fjerritslev formations according to Nielsen & Japsen (1991). Estimated uplift values based on Japsen et al. 2007.

	J-1	Flyvbjerg-1	Vedsted-1	Gassum-1	Thisted-3	Stenlille-6
Top Fjerritslev Fm Depth below msl. (m)	1074	997	1219	1140	987	1260
Top Gassum Fm Depth below msl. (m)	1697	1261	1744	1460	1093	1531
Base Gassum Fm Depth below msl. (m)	1808*	1457	2032	1590	>1208	1673
Thickness Fjerritslev Fm (m)	623	264	674	320	106	271
Thickness Gassum Fm (m)	111*	178	195	130	>130	142
Experienced post Early Cretaceous uplift (m)	800	~750	500	600	~500	600

New interpretations of depth and thickness given in Sharp deliverable report 4.1
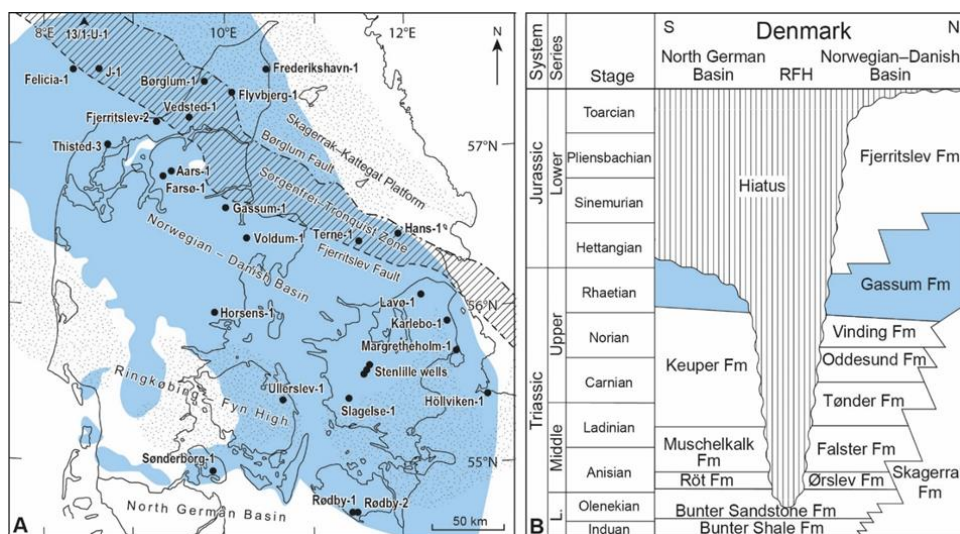

Figure 6-2 A) Structural elements and estimated distribution of the Gassum Formation in the Danish area shown in blue. B) Stratigraphic scheme of the Lower Triassic to Lower Jurassic succession onshore Denmark. From Olivarius et al. 2022.

<u>Comments to Lisa field</u>
There is no LOT data from the Lisa field, however, LOT data from Denmark has been plotted with depth in SHARP DV4.1 report. An updated plot of LOP data are shown in SHARP Report DV1.2, where LOT data points from Denmark are compared with trendlines for North Sea (Thompson et al., 2022b). Furthermore, the LOT data are grouped in the main groups Clay/Shales, Silt/Sandstones and Chalk. The LOP data are in good agreement with regional trendlines from the North Sea, and most LOP data plots within the expected variation range of expected lithological impact of a normally consolidated sediment K_0 =0.4-0.8 (as defined and discussed in this report). For further discussion of LOT data see Report DV1.2. The Danish stress data generally agree with trends from XLOT database in North Sea and Horda platform area.

The Fjerritslev sealing unit is dominated by kaolinite with some illite, mixed layer minerals, vermiculite and mica (not smectite), however details of Vclay are not available. Some information of Vclay and Vsmectite for Gassum formation are available from the Thisted 3 well North in Jutland, and Vclay and Vsmectite varies in range 22-64% and 0-5% respectively. Such values would give K_0 in a range 0.44 to 0.6 (by using Eq.15 in Table 5-1). Due to immature feldspar rich sand in the area of Lisa (Northwest Denmark), the clay contents and K_0 may be slightly higher than in Southeast. There is a significant uplift of ca 0.8 km in the Lisa structure. This corresponds to an OCR of ca. 1.5 at top Gassum Fm. sandstone reservoir. Present day depth of 1.55 km m BSF and maximum burial depth of ca 2.3 km. Some chemical alteration may therefore be relevant in both Gassum Fm. and the sealing Fjerritslev Fm. and the mechanical OCR effect from uplift, as seen for mudstones experienced shallower burial depth, may not be expected. If including impact of OCR by 1.5, by assuming no chemical alteration, the range of K_0 from normally consolidated (K_0 =0.44-0.60) to uplifted and overconsolidated would be 0.54 - 0.7 (by using Eq.15 in Table 5-1). There is also a shallow (ca 100 m thick) unit of Pleistocene sediments above chalk reported as gravel and sand (J-1x completion report). Presence of Oligogene Smectite rich sediments is not yet known for the Lisa profile, however presence of ca 20-30% Smectite and 30-40% Kaolinite (in % of clay fraction) is indicated from regional maps (see Figure 5-2). Whilst specific laboratory re-sedimentation data is not available for chalks as it is for sands and clays, K_0 triaxial testing of porous chalks, including Maastrichtian age chalk from Stevns Klint, Denmark with porosities >47%, reported by Omdal et al., 2010, indicate K_0 values generally between 0.45 and 0.51.

Although the Lisa structure is to be considered as a data poor case, it seems plausible that an initial strees profile may be obtained based on the mineralogical data and what can be extracted of knowledge and data from the data rich cases included in the present study. It should be emphazised that LOP data have uncertainties and individual LOP datapoints may vary from various reasons (Raaen et al., 2006), and we therefore recommend rather using the average trend for LOT datasets, and LOP data and especially outlayers should be quality checked if available to improve confidence. Like for Lisa, Felicia-1 well, LOP's close to Lisa deviates from average trendlines trend with high values. A further evaluation of the quality of these LOP data from the pumping pressure charts and the local stress field around Lisa structure would be beneficial for improved local confidence. For more discussion and limitations of using LOT data, see also discussion under DV1.2 (Chapter 6) and for more details see Raaen et al., 2006.
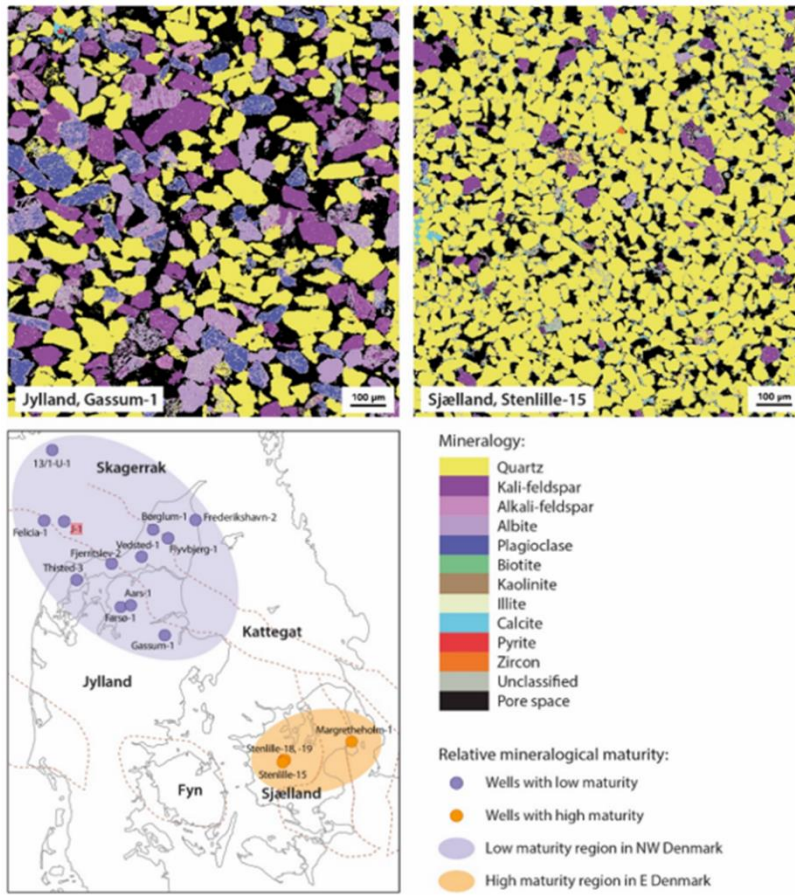
Figure 6-3 The mineralogical maturity of the Gassum Formation various across the Danish area and can be divided into a region of high maturity and low maturity, respectively (lower figure). The two sandstone samples are examples of the mineralogy from the region of low maturity (upper left) and the region of high maturity (upper right). From Olivarius 2022.
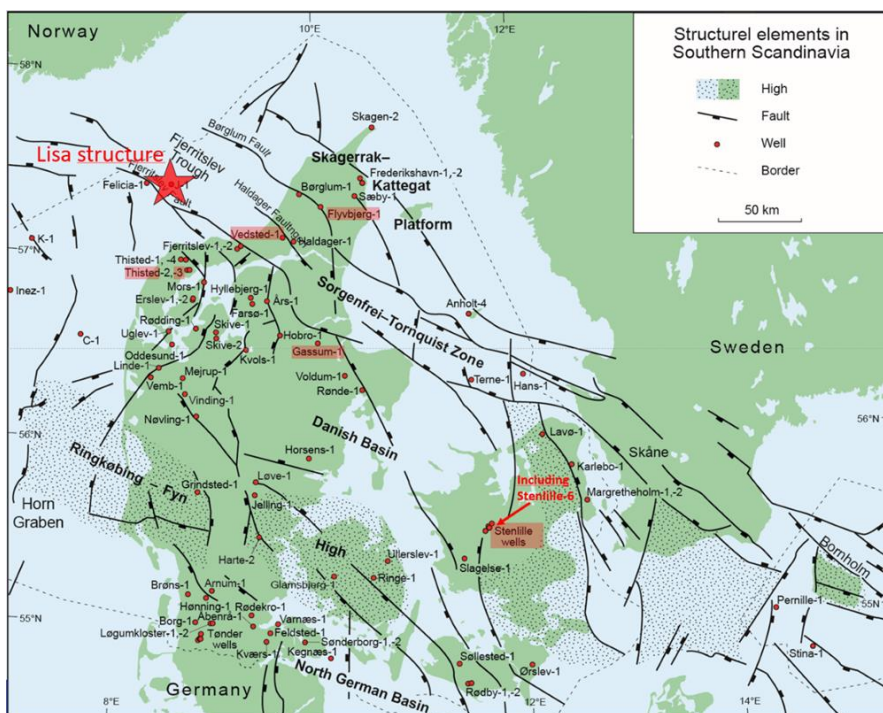

Figure 6-4 Marked wells are those from which core plugs from the Gassum Formation have been collected for the rock mechanical analysis. Structural map based on Nielsen (2003).
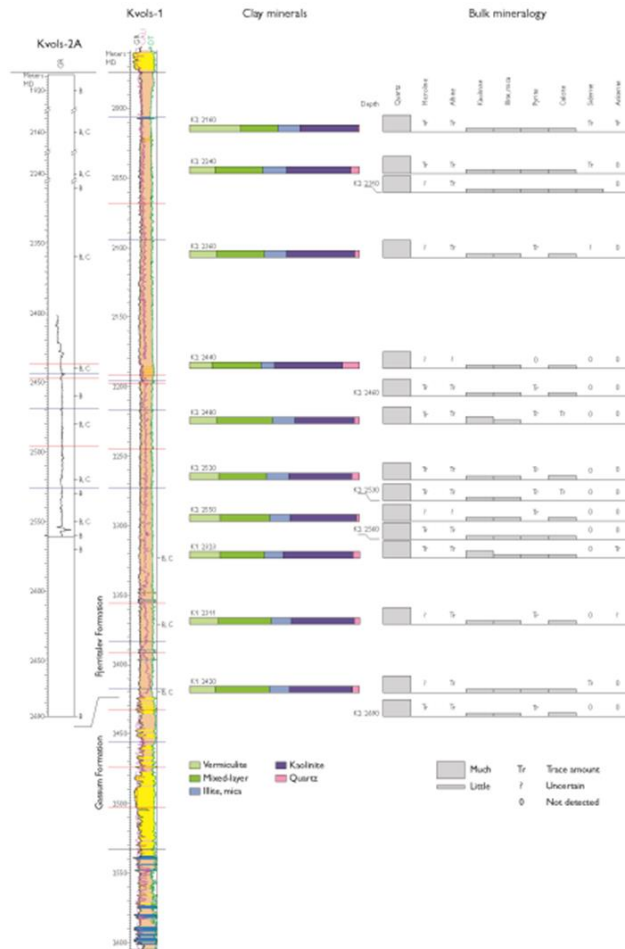
Figure 6-5 Bulk mineralogy, and clay minerals of the Fjerritslev Formation in the Kvovls-1, -2A wells. The wells are located in Northern Jutland (their location given by the Kvovls-1 well in Figure 4.3). From Vosgerau et al. (2016).

Figure 6-6 Stress orientations and well locations for 'A' to 'D' quality data. The symbols show the orientation of the maximum horizontal stress including the standard deviation. Yellow star marks approximately location of the Lisa structure. From Ask et al. 1996.

7 Summary and conclusion

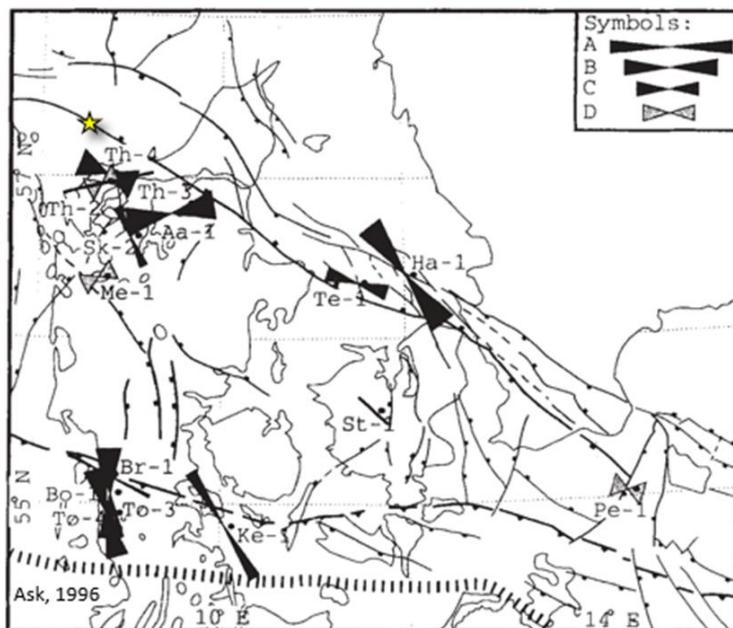This work is connected to other WPs, and the documented relationships and datasets are for further use in other SHARP tasks (WP1, 2, 3 and 5). Particularly, the result from this work is applied and further analysed under WP1, focusing on applications to logs, constitutive modelling, and calibration with field stress data. Details of this work and discussions on the impact of diagenesis and pore pressures are discussed under WP1 deliverables DV1.1b, DV1.2 and DV1.3. Whilst this report provides a comprehensive summary of activity to date, there is still much ongoing work. The remaining BGS tests (Chapter 4) will be reported and concluded in DV3.6 report towards the end of SHARP project (first half of 2024).

7.1 Laboratory test data and empirical correlations for K_0, constrained modulus and permeability.

In DV3.2 report, we have been focusing on experimental laboratory work to adress the impact of lithology and burial history on the present day state of stress. We have analysed existing databases, literature data and dedicated rock deformation experiments to develop empirical relationships between ratio of effective stress ratio (K_0), permeability and consolidation parameters vs. stress loading and unloading.

The existing and new empirical relations for K_0 have been tested with K_0 derived from field stress LOT and XLOT data in report DV1.2. A new procedure to link the empirical relationships for K_0 with gammaray log data were documented in Grande et al 2022, to incorporate depth dependent variabilities as a function of mineralogy and uplift. The log based method were tested for several wells in the Horda platform area where XLOT data are available. In summary estimated K_0 were found to be in good agreement for high quality XLOT tests and normally consolidated lithologies at entire depth of evaluation (0.6-2.3 km). For Shallow units (<0.6km), estimated K_0 using the OCR term can reproduce high K_0 from LOP values in Tertiary (Hordaland Gp).

7.1.1 Laboratory test data for K_0.

The following may be summarized from this report for the effective stress ratio (K_0);

- Various empirical relations relating K_0 to mineralogy and overconsolidation ratio have been summarised from the literature, and new relations based on content of clay (V_{cl}) and smectite ($V_{smectite}$), plasticity index (I_p) have been further developed based on geotechnical and rock mechanical datasets from Troll and Oseberg area.
- K_0 tests in natural clays, mudstone and cemented shales have been compared with clay data. Stabilized values of K_0 at very high effective stress is believed to vary within the same range as for normally consolidated K_0 for sediments. However, several studies reporting K_0 values from tests in rock have low values and have not reached the normally consolidated state (beyond pseuedo-pre consolidation from cementation).
- The observed range of K_0 from laboratory data on synthetic and natural sand, silt, clay and mudstone and shales of ca 0.4-0.8 defines the expected natural variation in K_0 for the normally consolidated state of sediments undergoing uniaxial compaction. This was demonstrated from using friction angle of

remoulded sediments, plasticity, and content of clay in several independent studies.

- Behaviour of K_0 in shales during unloading from literature is not consistent, and poorly understood. In this report we show for a mudstone that the behaviour during unloading are similar for sands and clays with K_0 increasing as a function of overconsolidation ratio (OCR). However, new examples of a cemented shale show constant K_0 during unloading. This indicates a behaviour more in line with previous observations from the literature where K_0 has decreased during unloading (Berre et al. 1996).
- Relations for constrained modulus and permeabilities of clays, mudstones and shales were investigated, compared and reported. These may be useful input to consolidation modelling of stress history and evaluation of load vs. time and drained vs. undrained behaviour of clays and shales (i.e over pressured units).

7.1.2 Testing experimental data and empirical relation with field stress data sets

The following may be summarized base on updated work under DV3.2

- The range of K_0 of ca 0.4-0.8 observed from normally consolidated sediments in laboratory are in line with range of K_0 from high-quality XLOT stress tests in the Norwegian continental shelf and in the Horda platform area (Andrews, 2016, Thompson et al., 2022a and 2022b).
- The empirical relations were demonstrated using mineralogy data for reference lithologies in the Horda platform and compared K_0 derived from XLOT in a few intervals, where estimated K_0 value of the normally consolidated sediment compares well with K_0 from XLOT (within +/-10%). However, measured values in uplifted Drake (Eos) and Draupne (Smeaheia) are lower than expected from mineralogy.
- For normally consolidated clay, mudstone and shale reservoir level, we suggest that at a range of K_0=0.6+/-0.2 would adequately bracket the lithologiacal impact of normally consolidated state. Average trend of K_0 of ca 0.6 and 0.63 from laboratory data and XLOT data in the North Sea (Thompson et al 2022b) and average, correspond to normally consolidated sedimets with V_{cl} of 67 to 76% in-line with Draupne V_{cl} in Smeaheia. Heather formation have lower values of V_{cl} of 45% corresponding to K_0 of 0.52
- For uplifted shallow lithologies, evidence from Quaternary clays and Tertiary mudstones indicates K_0 ca 0.6-1, in agreement with the OCR term, however the effect of OCR is likely be limited to a depth somewhere in transitions from mudstone to shale (i.e. 1-2 km). Laboratory experiment on mudstone (<1 km dept) show increased K_0 under unloading.
- For uplifted deeper cemented lithologies such as Drake and Draupne K_0 from field stress data (XLOT) mainly show no increase of K_0 when uplifted, however, considering LOP data there are exceptions like Draupne in Smeaheia Beta indicating higher values of K_0. The K_0 for deep shale tested was not changed significantly from unloading. For discussion of K_0 and diagenetic processes is see discussion in report DV1.2 and DV1.3 report.
- For Draupne fm. the calculated K_0 are in range 0.57-0.63 based on friction angles in range 18.8-22.3° as measured on reconstituted Draupne shale from Ling depression and K_0 of 0.62 and 0.55 were calculated from Ip and V_{cl} and $V_{smectite}$. These are close to K_0 of 0.63 and 0.54 are reported based on XLOT tests in Eos well and Smeaheia gamma well respectively.

- For Drake fm. a reconstituted sample (crushed to powder) were tested in DST under SHARP. The calculated value of K_0 was 0.51 from both the measured friction angle of 25.8° and the plasticity Ip of 13% and calculated K_0 was 0.6 based on V_{cl} of 61% and from XRD data from same core (using $V_{smectite}$ of 10%). Calculated average value of K_0 for NC state is 0.54, only 1.8% less than the high end value of K_0 =0.55 reported from XLOT.
- Lithological bounds of K_0 for the lithological impact on stress has demonstrated for all the SHARP sites in the North Sea (in report DV1.2) in combination with previously published regional stress trends for North Sea (Thompson et al., 2022) and these trends cover all datapoins from XLOT data in Horda and LOP available for SHARP study from Denmark.

7.1.3 Limitations in database on K_0 and uniaxial strain assumtion

- This study focuses on siliciclastic sediments, including clay, sand, and mudstones and shales dominated by clay minerals illite, kaolinite, smectite and quarts. Other lithologies like halite, chalks and other carbonate-rich sediments are not analysed herein. However, lithological effects on the LOP data are indicated for Danish chalks and UK Halites. Other relations may be valid for such formation, especially for Halite which behaves viscoplastically when subjected to stress and temperature, resulting in a K_0 close to 1 (Williams, 2015).
- This study focuses on relationships based on mechanical compaction and uniaxial strain assuming relaxed basins. Inspite of the complex tectonic history of North Sea basins (periods of exposure to extensional/compressional stress fields, inversions/uplifts) and the likely activity of time/temperature dependent mechanical and chemical creep, pressure and dissolution processes, the K_0 derived from XLOT data often falls within the expected range of K_0 based on lithological variations under conditions of uniaxial strain.

7.2 K_0 testing and numerical modelling Quaternary sediments

The following may be summarized from this report for the K_0 testing and modelling in Quaternary sediments.

- Understanding stress history and lithological properties within the shallow units, that are much more accessible, has demonstrated to be of great value. They can give good clues to stress responses much deeper, assuming we have some decent understanding of the geology and mineralogy.
- From four new laboratory K_0 test on Onsøy material, simlulating glacial loading and unloading at both Onsøy and Troll, the K_0 of 0.88 derived from Onsøy unloading phase is in range of K_0 from Onsøy field measurements. The range of K_0 (0.81-0.88) from Troll unloading phase is close to the predicted in range of recommended values of K_0 of 0.8-0.9 for Troll Unit IV based on empirical correlations.
- Result from numerical simulations (Plaxis) using HVMCC model for Troll Unit III give larger values of K_0 ($K_0 \approx 1$) compared to the SSC model ($K_0 \approx 0.8$), however, both values are lower than recommended K_0 of 1.2 from empirical correlations. In cases of large unloading, these numerical approaches cannot mimic results from previous laboratory studies and corresponding empirical correlations. (i.e. from laboratory data, $K_0 > 1$ when OCR>ca 3-5).

7.3   Permeability testing in UK analogue sandstones

The following may be summarized from this report for the relationships of the permeability test on cemented sandstone.

- For new tests on UK sandstones, there are significant stress dependencies on the permeabilityunder gradually increasing isotropic stress, which is different during unloading compared to loading.
- The remaining of BGS tests (Chapter 4) will be reported and concluded in DV3.6 report towards end of SHARP project in first half of 2024.

7.4   Conclusions

The following may be concluded from this report at this stage of the SHARP project.

- New datasets from natural clays, mudstones and shales to assess the lithology and stress history impacts on in-situ stress has been included in correlations, constitutive models and numerical simulations. The new data and correlations focuses for effective stress ratio (K_0), permeability and modulus for use in correlations and constitutive models for numerical analysis.
- Existing and new correlations and workflow to adress the K_0 from mineralogical data have been developed, refined in this report and DV1.2 report, and the range of K_0 determined from these correlations based on lithological variations corresponds well with observed variation range from field XLOT stress data in North Sea .
- A workflow to assess K_0 and minimum horizontal stress has been tested and demonstrated for Lisa and Hordaplatform lithologies, and these can be applied in various stages of CO2 developments., i.e in early stage when only limited geological information and LOT data are available or for a more detailed assessment when logs and cores are available in combination with XLOT and LOT data.
- New K_0 laboratory tests from Onsøy soft clay with unloading simulate the measured K_0 from in-situ field stress in Onsøy and the empirically derived K_0 in Troll reasonably well. Numerical model simulating impact of glacial loading in Troll are similar to empirically derived K_0, exeptions is for highly overconsolidated Troll Unit III where results from HVMCC and SSC model are lower than the empirically derived K_0.
- New tests for analoge UK sandstone samples, show significant stress dependencies on the permeability under gradually increasing isotropic stress, which is different during unloading compared to loading.

8   References

Aas G, Lacasse S, Lunne T, et al. (1986) Use of in situ tests for foundation design on clay. Use of In Situ Tests in Geotechnical Engineering, 1–30.

Andrews, J., Fintland, T., Helstrup, O., Horsrud, P., Raaen, A., 2016. Use of unique database of good quality stress data to investigate theories of fracture initiation, fracture propagation and the stress state in the subsurface. 50th U.S. Rock Mechanics/Geomechanics Symposium, American Rock Mechanics Association.

Andrews J., and de Lesquen C., 2019, Stress determination from logs. Why the simple uniaxial strain model is physically flawed but still gives relatively good matches to high quality stress measurements performed on several fields offshore Norway, 53rd US Rock Mechanics/Geomechanics Symposium held in New York, NY, USA, 23–26 June 2019.

Ask, M. V., Müller, B., & Stephansson, O. (1996). In situ stress determination from breakouts in the Tornquist Fan, Denmark. Terra Nova, 8(6), 575-584.

Baud P, Vajdova V, Wong T-F. (2006) Shear-enhanced compaction and strain localization: Inelastic deformation and constitutive modeling of four porous sandstones. Journal of Geophysical Research: Solid Earth. 2006; 111: B12

Baud, P., Klein, E. and Wong, T.F. (2004) Compaction localization in porous sandstones: spatial evolution of damage and acoustic emission activity. Journal of Structural Geology, 26(4), pp.603-624.

Berre, T., Tunbridge, L. and Høeg, K., 1995, The measurement of small strains and K_0 values in Triaxial tests on clay-shales. In 8th International, Congress on Rock Mechanics, 25-29 Sept. , Chiba, Japan

Bertelsen, F. 1978. The Upper Triassic – Lower Jurassic Vinding and Gassum Formations of the Norwegian–Danish Basin. Danmarks Geologiske Undersøgelse Serie B, Nr. 3, 26 pp. https://geusjournals.org/index.php/serieb/issue/view/927

Bjørløkke, K and Høeg, K., (1997), Effects of burial diagenesis on stresses, compaction and fluid flow in sedimentary basins, Marine and Petroleum Geology, Vol. 14, No 3, pp. 267-276

Bjerrum L, Andersen KH (1972) In-situ measurement of lateral pressures in clay. Nor Geotech Inst Publ, 29–38.

Bjørlykke, K., 1998, Clay mineral diagenesis in sedimentary basins-a key to the prediction of rock properties. Examples from the North Sea Basin, Clay Minerals 33, page 15-34

Brooker E.W and Ireland, H.O., (1965), Earth pressure at rest related to stress history. Canadian Geotechnical Journal, 2(1), 15

Cuss R.J, Rutter, EH, and Holloway, RF (2003) The Application of Critical State Soil Mechanics to the Mechanical Behaviour of Sandstone. Int. J. of Rock Mech. and Min. Sci. 2003; 40: 847-62. DOI: 10.1016/S1365-1609(03)00053-4

Casagrande, A., 1936, The determination of the pre-consolidation load and its practical significance, Proceedings of the international conference on soil mechanics and foundation engineering. Vol. 3. Harvard University Cambridge. pp. 60–64.

Dafalla, M. A. (2013). Effects of clay and moisture content on direct shear tests for clay-sand mixtures. Advances in Materials Science and Engineering, 2013.

Da Silva D. C. A, 2021, Experimental study addressing fault slip, Implications for derisking of the Smeaheia potential CO2 storage site, Master Thesis University of Oslo.

Davood D.A., Grimstad G., Ghoreishian Amiri S.A., 2022, On the isotache viscous modelling of clay behaviour using the hyperplasticity approach, Géotechnique, ISSN 0016-8505 | E-ISSN 1751-7656

Downing RA, Burgess WG, Smith IF, Allen DJ, Price M and Edmunds WM (1982). Investigation of the geothermal potential of the UK; Geothermal aspects of the Larne No 2 Borehole London Institute of Geological Science NERC report.

Fawad, M., N. H. Mondol, J. Jahren, and K. Bjørlykke, 2011, Mechanical compaction and ultrasonic velocity of sands with different texture and mineralogical composition: Geophysical Prospecting, 59, no. 4, p. 697- 720.

Faulkner, D.R. and Rutter, E.H.(2000) Comparisons of water and argon permeability in natural clay-bearing fault gouge under high pressure at 20° C. Journal of Geophysical Research: Solid Earth, 105(B7), pp.16415-16426.

Fischer,G . J., and M. S Paterson (1992) Measurement of permeability and storage capacity in rocks during deformation at high temperature and pressure. In Fault Mechanics and Transport Properties of Rocks, and T.-f. Wong, pp. 213-251, Academic, San Diego, Calif., 1992. edited by B. Evans.

Fortin, J., Stanchits, S., Dresen, G. and Guéguen, Y. (2006) Acoustic emission and velocities associated with the formation of compaction bands in sandstone. Journal of Geophysical Research: Solid Earth, 111(B10).

Frikha, W., & Jellali, B. (2017). Numerical and experimental studies of sand-clay interface. International Congress and Exhibition" Sustainable Civil Infrastructures: Innovative Infrastructure Geotechnology", 108-120.

Grande, L., Berre, T and Mondol, N. H., 2011, Horizontal stress development in fine-grained sediments and mudstones during compaction and uplift, 73rd EAGE Conference & Exhibition incorporating SPE EUROPEC 2011

Grande L, Griffith L., Choi,J.C., Mondol N.H., 2022, Dynamic versus static modulus in clays and mudstones in the North Sea, 6th International Workshop on Rock Physics 13 – 16 June 2022, A Coruña, Spain

Grande, L., and N.H. Mondol, 2013, Geomechanical, hydraulic and seismic properties of unconsolidated Sediments and their applications to shallow reservoirs, American Rock Mechanics Association (ARMA) Conference, San Francisco 24-26 June 2013, Paper ARMA 13-536

Grande, L., Mondol, H. N., Skurtveit, E., Thompson, N., 2022, Stress estimation from clay content and mineralogy-Eos well in the Aurora CO_2 storage site, offshore Norway, 16th International Conference on Greenhouse Gas Control Technologies, GHGT-16 23rd -27th October 2022, Lyon, France

Grande L.,Forsberg C.,F-. Mondol N., , Skurtveit E., Singh R.M., Ghoreishian Amiri S.A., Jalali R, Thompson N., Roberts D., Phillips D., 2023, Impact of sediment composition, glacial loading and uplift on ground stresses in the Horda-Platform area, TCCS-12 Trondheim

Grimstad, G., Long, M., Dadrasajirlou, D., and Amiri, S. A. G., 2021,"Investigation of Development of the Earth Pressure Coefficient at Rest in Clay During Creep in the Framework of Hyper-Viscoplasticity," International journal of geomechanics, vol. 21, no. 1, 2021, doi: 10.1061/(ASCE)GM.1943- 5622.0001883.

Gundersen, A.S., Hansen, R.C., Lunne, T., L'Heureux, J.-S., & Strandvik, S.O., 2019, Characterization and engineering properties of the NGTS Onsøy soft clay site, AIMS Geosciences, 5(3):665-703. doi:10.3934/geosci.2019.3.6

ISO (2012) Geotechnical investigation and testing—Field testing. Part 5: Flexible dilatometer test (ISO 22476-5). Geneva, Switzerland: International Organization for Standardization.

Harrington, J.F., Graham, C.C., Dobbs, M., Cuss, R.J., Daniels, K.A., Wiseall, A.C., Parkes, D., Paluszny, A., Zimmerman, R.W., Salimzadeh, S., Tsaparli, V., Tempone, P., Thomas, R.N., Xenias, D., And Whitmarsh, L. (2018) CONTAIN D11: Integrated final results and conclusions. CONTAIN Report D11, 72pp.

Holt R.M.,; Brignoli. M.,; Fjaer. E.,; Unander T.E.,; Kenter C.J, 1994, Core damage effects on compaction behaviour, Paper presented at the Rock Mechanics in Petroleum Engineering, Delft, Netherlands, August 1994, Paper Number: SPE-28027-MS, https://doi.org/10.2118/28027-MS

Hoek E, Carranza-Torres C, Corkum B. Hoek-Brown (2002) Failure Criterion – 2002 Edition. In: Proceedings of the. NARMS-TAC Conference. University of Toronto, Toronto; 10 July 2002. pp. 267–73.

Hoek E, Diederichs MS (2006) Empirical estimation of rock mass modulus. Int. J. of Rock Mech. & Min. Sci. 2006; 43: 203–15

Ikari, M. J., Saffer, D. M., & Marone, C. (2009). Frictional and hydrologic properties of clay-rich fault gouge. Journal of Geophysical Research: Solid Earth, 114(B05409), 1-18. https://doi.org/doi:10.1029/2008JB006089

Jalali, R., 2022, Consolidation and stress history in shallow sediments in the northern North Sea, Master thesis NTNU

Janbu, N. 1969. The resistance concept applied to deformation of soils. In Proceedings of the 7th International Conference on Soil Mechanics and Foundation Engineering, Mexico City, 25–29 August 1969. A.A. Balkema, Rotterdam, the Netherlands. Vol. 1, pp. 191–196.

Jaky, J. (1944), "The Coefficient of Earth Pressure at Rest" (in Hungarian), Journal Society of Hungarian Architects and Engineers, Budapest, Hungary. pp. 355-358.

Japsen, P., Green, P. F., Nielsen, L. H., Rasmussen, E. S., & Bidstrup, T. (2007). Mesozoic–Cenozoic exhumation events in the eastern North Sea Basin: a multi-disciplinary study based on palaeothermal, palaeoburial, stratigraphic and seismic data. Basin Research, 19(4), 451-490.

Kenney, T. C. (1959). Discussion of "Geotechnical properties of glacial lake clays" by T. H. Wu. . Soil Mech. and Foundations Div., ASCE, 85(3), 67-79.

Klein, E., Baud, P., Reuschlé, T. and Wong, T.F. (2001) Mechanical behaviour and failure mode of Bentheim sandstone under triaxial compression. Physics and Chemistry of the Earth, Part A: Solid Earth and Geodesy, 26(1-2), pp.21-25.

Kranz, R. L., J. S. Saltzman, and J. D. Blacic (1990) Hydraulic diffusivity measurements on laboratory rock samples using an oscillating pore pressure method. Int. J. Rock. Mech. Min. Sci. Geomech. Abstr., 27, 345-352, 1990.

Louis, L., Baud, P. and Wong, T.F. (2009) Microstructural inhomogeneity and mechanical anisotropy associated with bedding in Rothbach sandstone. Pure and applied geophysics, 166(5-7), pp.1063-1087.

L'Heureux, J-S; Ozkul, Z; Lacasse, S; D'Ignazio, M; Lunne, T, 2017, Bestemmelse av hviletrykk (K0) i norske leirer – anbefalinger basert på en sammenstilling av lab-, felt- og erfaringsdata, Fjellsprengningsteknikk - bergmekanikk - geoteknikk. Oslo 2017. Lecture 35. English Title: "Determination of the earth pressure at rest (K0)-in Norwegian clays-recommendations based in lab-, field, and experience data"

Lunne, T., Long, M., and Uzielli., M, 2006, Characterisation and engineering properties of Troll clay, Proceedings Workshop in Singapore Nov. 06

Lunne T, Powell JJ, Robertson PK (1997) Cone penetration testing in geotechnical practice. CRC Press.

Lunne, T., Long M., and Forsberg C.F., 2002, Characterization and engineering properties of Onsøy clay

Massarsch, K.R. (1979). "Lateral earth pressure in normally consolidated clay". In Design parameters in geotechnical engineering. BGS, London. Vol. 2.

Mayne P, Kulhawy FH (1982) K0–OCR relationships in soil. J Geotech Eng Div 108: 851–872.

Mayne, P. W., and Kulhawy, F. H. (1990). "Direct and indirect determinations of in situ K0 in clays". Transportation Research Record, (1278).

Marsland A, Randolph MF (1977) Comparison of the results from pressuremeter tests and large in situ plate tests in London Clay. Géotechnique 27: 455–477.

Marcussen, Ø., Faleide, J. I., Jahren, J., & Bjørlykke, K. (2010). Mudstone compaction curves in basin modelling: a study of Mesozoic and Cenozoic Sediments in the northern

North Sea. Basin Research, 22(3), 324–340. https://doi.org/10.1111/j.1365-2117.2009.00430.x

Mesri, G., and Hayat, T.M., (1993), The coefficient of earth pressure at rest, Canadian Geotechnical Journal, 30(4), 647 – 666.

Marchetti S, Monaco P, Totani G, et al. (2001) The flat dilatometer test (DMT) in soil investigations. A report by the ISSMGE Technical Committee 16 on Ground Property Characterisation from In-situ Testing. International Conference on Insitu Measurement of Soil Properties. Bali, Indonesia, 95–131.

Marchetti S (1980) In situ tests by flat dilatometer. J Geotech Eng Div 106: 299–321.

Meneguolo, R., Hellevang, H., Sundal, A., Thompson, N., 2021, Muti-scale cap rock assessment for CO2 storage, insights fom the Northern Lights project (Norwegian Continental Shelf). Basin and Petroleum Systems Modelling: Best Practices, Challenges and New Techniques, The Geological Society, 28-30 September, London.

Michelsen, O., Nielsen, L.H., Johannessen, P.N., Andsbjerg, J. and Surlyk, F. 2003. Jurassic lithostratigraphy and stratigraphic development onshore and offshore Denmark. In: Ineson, J.R. and Surlyk, F. (eds): The Jurassic of Denmark and Greenland. Geological Survey of Denmark and Greenland Bulletin 1, p. 145–216. https://doi.org/10.34194/geusb.v1.4651.

Mondol, N.H., Grande. L., Bjørnarå T.I., and Thompson. N., 2022, Caprock characterization of the Northern Lights CO2 storage project, offshore Norway, EAGE GeoTech 2022, 4-6 April 2022

Mayne, P. W., and Kulhawy, F. H. (1990). "Direct and indirect determinations of in situ K0 in clays". Transportation Research Record, (1278).

Mondol, N.H., 2009. Porosity and permeability development in mechanically compacted silt-kaolinite mixtures, in: SEG Technical Program Expanded Abstracts 2009. Society of Exploration Geophysicists, pp. 2139–2143.

Nielsen, L.H. 2003. Late Triassic – Jurassic development of the Danish Basin and the Fennoscandian Border Zone, southern Scandinavia. In: Ineson, J.R. and Surlyk, F. (eds): The Jurassic of Denmark and Greenland. Geological Survey of Denmark and Greenland Bulletin 1, p. 459–526. https://doi.org/10.34194/geusb.v1.4681.

Nielsen, L.H. & Japsen, P. 1991. Deep wells in Denmark 1935-1990. Lithostratigraphic subdivision. Danmarks Geologiske Undersøgelse, DGU Serie A, No. 31, 177 pp.

Narongsirikul, S., N. H. Mondol, and J. Jahren, 2020, Effects of stress reduction on geomechanical and acoustic relationship of overconsolidated sands, Geophysical Prospecting, Vol 68, No 3, March 2020, pp. 968 – 981, DOI: 10.1111/1365- 2478.12902

NGI 1990, HYDRAULIC FRACTURE AND CONDUCTOR INSTALLATION COLLATION AND ANALYSIS OF FIELD TESTS, Tom Lunne and Trond By, NGI Report 521620-2 10 December 1990

Noy, D.J.; Holloway, S.; Chadwick, R.A.; Williams, J.D.O.; Hannis, S.A.; Lahann, R.W (2012) Modelling large-scale carbon dioxide injection into the Bunter Sandstone in the UK Southern North Sea. International Journal of Greenhouse Gas Control, 9. 220-233.

Nygård, R., Gutierrez, M., Gautam, R., Høeg, K., (2004), Compaction behavior of agillaceous sediments as function of diagenesis, Marine and Petroleum Geology (21) 349-362

Olivarius, M., Vosgerau, H., Nielsen, L.H., Weibel, R., Malkki, S.N., Heredia, B.D. and Thomsen, T.B. 2022. Maturity Matters in Provenance Analysis: Mineralogical Differences Explained by Sediment Transport from Fennoscandian and Variscian Sources. Geosciences 2022, 12(8), 308. 24 pp. https://doi.org/10.3390/geosciences12080308.

Parkes D, Graham C C, Harrington J F, Cuss R J, Ougier-Simonin A, (2014). CONTAIN D1: Identification of candidate geologies and experimental approach. British Geological Survey Open Report, OR/15/008. 93pp.

Peltonen, C., Marcussen, Ø., Bjørlykke, K., Jahren, J., 2009, Clay mineral diagenesis and quartz cementation in mudstones: the effects of smectite to illite reaction on rock properties, Mar. Pet. Geol., 26 (2009), pp. 887-898.
Huggett J.M. (1992) Petrography, mineralogy and diagenesis of overpressured Tertiary and Late Cretaceous mudrocks from the East Shetland, Basin. Clay Miner. 27, 487-506.

Rahman, J.,Fawad, M., Mondol N.H., 2020, Organic-rich shale caprock properties of potential CO2 storage sites in the northern North Sea, offshore Norway, Marine and Petroleum Geology 122 (2020) 104665.

Rahman, M.J., Fawad, M., Jahren, J. Mondol, N.H. 2022. Influence of Depositional and Diagenetic Processes on Caprock Properties of CO2 Storage Sites in the Northern North Sea, Offshore Norway. Geosciences, 12, 181. https://, doi.org/10.3390/geosciences12050181.

Rutter, E.H. and Glover, C.T. (2012) The deformation of porous sandstones; are Byerlee friction and the critical state line equivalent?. Journal of Structural Geology, 44, pp.129-140.

Roberts, D. T., A. J.L. Crook, J. A. Cartwright, M. L. Profit, and J. M. Rance. 2014. "The Evolution of Polygonal Fault Systems: Insights from Geomechanical Forward Modeling." 48th US Rock Mechanics / Geomechanics Symposium 2014 1 (May 2016): 488–502

Rundberg Y. (1989) Tertiary sedimentary history and basin evolution between 60628; an integrated approach. Dr. Eng. thesis, Univ. Trondheim, Norway

Simpson, D., & Evans, T. (2016). Behavioral thresholds in mixtures of sand and kaolinite clay. Journal of Geotechnical and Geoenvironmental Engineering, 142(2), 04015073.

Soldal, M.; Skurtveit, E.; Choi, J.C., 2021, Laboratory Evaluation of Mechanical Properties of Draupne Shale Relevant for CO2 Seal Integrity. Geosciences 2021, 11, 244. https:// doi.org/10.3390/geosciences11060244

Thompson, N., Andrews J.S., Wu, L., Meneguolo, R., 2022, Characterization of the in-situ stress on the Horda platform – A study from the Northern Lights Eos well, International Journal of Greenhouse Gas Control 114 (2022) 103580

Valle Kopperud and Tubid Myhrvold, 2023, NTNU Master thesis, submitted June 2023.

Vosgerau, H., Gregersen, U., Hjuler, M.L., Holmslykke, H.D., Kristensen, L., Lindström, S., Mathiesen, A., Nielsen, C.M., Olivarius, M., Pedersen, G.K. and Nielsen, L.H. 2016. Reservoir prognosis of the Gassum Formation and the Karlebo Member within two areas of interest in northern Copenhagen. The EUDP project "Geothermal pilot well, phase 1b". GEUS Rapport 2016/56. 138 pp + app 1–5. https://doi.org/10.22008/gpub/32477

Wangen, M. 2000. "Generation of Overpressure by Cementation of Pore Space in Sedimentary Rocks." Geophysical Journal International 143: 608–20.

Wong T-F, David C, Zhu W (1997) The transition from brittle faulting to cataclastic flow in porous sandstones mechanical deformation. J. Geophys. Res. B. 1997; 102(2): 3009–25.

Wong, T.F. and Baud, P. (2012) The brittle-ductile transition in porous rock: A review. Journal of Structural Geology, 44, pp.25-53.

Wu, L., Skurtveit, E., Thompson, N., Michie, E., Fossen, H., Braathen, A., Fisher, Q., Lidstone, A., and Bostrøm, B., 2022, Contaiment Risk Assessment and Management of CO2 storage on the Horda platform, 16th International Conference of Greenhouse Gas Control Technologies, GHGT-16, 23rd-27th October 2022, Lyon, France.

Zhu W, Wong T-F (1997) Shear-enhanced compaction in sandstone under nominally dry and water-saturated conditions. Int. J. Rock Mech. Min. Sci. 1997; 34: 372.